

* Vector meson exchange contributions to

$$K \rightarrow \pi\gamma\gamma \text{ and } K_L \rightarrow \gamma\ell^+\ell^-$$

Giancarlo D'Ambrosio[†] and **Jorge Portolés[‡]**

Istituto Nazionale di Fisica Nucleare, Sezione di Napoli
Dipartimento di Scienze Fisiche, Università di Napoli
I-80125 Napoli, Italy

Abstract

We have studied in the framework of Chiral Perturbation Theory (χ PT) the $\mathcal{O}(p^6)$ Vector Meson contributions to $K \rightarrow \pi\gamma\gamma$ and $K_L \rightarrow \gamma\gamma^*$. We construct the most general χ PT lagrangian for the weak Vector–Pseudoscalar–Photon ($VP\gamma$) vertex for $K \rightarrow \pi\gamma\gamma$ and $K_L \rightarrow \gamma\gamma^*$ and consequently we get the full structure of the $\mathcal{O}(p^6)$ local contributions generated by Vector Meson exchange. Then we compute new factorizable contributions to the weak $VP\gamma$ vertex generated by the odd–intrinsic parity violating lagrangian with no additional couplings. We find in fact a very nice agreement with the phenomenology of $K \rightarrow \pi\gamma\gamma$ and $K_L \rightarrow \gamma\gamma^*$, more predictive power and a deeper understanding of the $\mathcal{O}(p^6)$ local operators. A novel interpretation of the $K_L \rightarrow \gamma\gamma^*$ data is given. Also a comparison with the existing models is presented.

PACS : 12.15.-y, 12.39.Fe, 12.40.Vv, 13.25.Es

Keywords : Radiative non–leptonic kaon decays, Non–leptonic weak hamiltonian, Chiral Perturbation Theory, Vector meson dominance.

[†] E-mail : dambrosio@na.infn.it

[‡] E-mail : portoles@axpna1.na.infn.it

* Work supported in part by HCM, EEC–Contract No. CHRX–CT920026 (EURODAΦNE).

1 Introduction

Our knowledge of the phenomenology of radiative non-leptonic kaon decays both from theoretical and experimental points of view has improved drastically in the last ten years. The main tool that has ushered this progress has been the application of Chiral Perturbation Theory (χ PT) [1, 2, 3] techniques to weak processes. χ PT is a quantum effective theory that satisfies the basic chiral symmetry of QCD and supports a perturbative Feynman–Dyson expansion in masses and external momenta. Correspondingly at any new order in the expansion new chiral invariant operators, with coupling constants not determined by the symmetry, appear. At $\mathcal{O}(p^4)$ vector meson exchange (when present) has been shown to be effective in predicting those couplings in the strong sector [4, 5]. This is not an easy task, however, in the weak lagrangian since the weak couplings of vector mesons are much less known. Thus various models implementing weak interactions at the hadronic level have been proposed, yet it is very likely that mechanisms and couplings working for a subset of processes might not work in general for other processes. Nevertheless the information provided by the models can be useful in giving a general picture of the hadronization process of the interaction.

χ PT has been successfully used to study radiative non-leptonic kaon decays (see [6, 7, 8] and references therein). Here we are concerned in the study of the $\mathcal{O}(p^6)$ vector meson exchange contributions to $K_L \rightarrow \gamma \ell^+ \ell^-$, $K_L \rightarrow \pi^0 \gamma \gamma$ and $K^+ \rightarrow \pi^+ \gamma \gamma$ decays.

The $K_L \rightarrow \gamma \gamma^*$ form factor (together with $K_L \rightarrow \gamma^* \gamma^*$) is an important ingredient in order to evaluate properly the dispersive contribution to the real part of the amplitude for the decay $K_L \rightarrow \gamma^* \gamma^* \rightarrow \mu^+ \mu^-$. Since the real part receives also short distance contributions proportional to the CKM matrix element V_{td} [9] and the absorptive amplitude is found to saturate the experimental result, a strong cancellation in the real part between short and long distance contributions is expected. Analysis of the relevant form factor in $K_L \rightarrow \gamma \gamma^*$ [10] shows a relatively large weak $\mathcal{O}(p^6)$ vector meson contribution and, therefore, it is of concern for our study here.

The importance of $K_L \rightarrow \pi^0 \gamma \gamma$ goes further the interest of the process in itself because its role as a CP-conserving two-photon discontinuity amplitude to $K_L \rightarrow \pi^0 e^+ e^-$ in possible competition with the CP-violating contributions [11, 12, 13]. The leading $\mathcal{O}(p^4)$ χ PT amplitude to $K_L \rightarrow \pi^0 \gamma \gamma$, which does not receive any local contribution, though predicting well the diphoton invariant mass spectrum, underestimates by a factor 3 the rate. No complete $\mathcal{O}(p^6)$ computation has been made; however, there are large unitarity corrections [14, 15] and one could fix the weak coupling carrying the information of the vector meson exchange to reproduce rate and spectrum [15]. This weak vector coupling also turns out to be large and it is not well explained by the theoretical models that have been used until now.

The interest on $K^+ \rightarrow \pi^+ \gamma \gamma$ relies also on its actuality. BNL-787 has got, for the

first time [16], 31 preliminary events on this channel and KLOE at DAΦNE will do in the near future. This good experimental perspectives will give information about the $\mathcal{O}(p^4)$ weak counterterms in the chiral lagrangian since now the $\mathcal{O}(p^6)$ unitarity corrections have already been evaluated [17]. At this chiral order is then necessary to have a control of the vector exchange contributions.

The interplay between experimental results and phenomenology indicates that in both these decays ($K \rightarrow \pi\gamma\gamma$ and $K_L \rightarrow \gamma\gamma^*$) there is an important $\mathcal{O}(p^6)$ vector meson exchange contribution, which prediction, as commented above, relies on theoretical models. We will review them in the paper. Let us collect here their main achievements :

- i) Weak Deformation Model (WDM) [18, 19] .- It might reproduce well the $K_L \rightarrow \gamma\gamma^*$ slope but gives a too small vector meson contribution to $K_L \rightarrow \pi^0\gamma\gamma$.
- ii) Factorization Model (FM) [20].- Motivated by $1/N_c$ models can give a consistent picture of both $K_L \rightarrow \pi^0\gamma\gamma$ and $K_L \rightarrow \gamma\gamma^*$, according to experiment, if the effective coupling (a free parameter in this model) is carefully chosen as we will show.
- iii) Bergström–Massó–Singer model (BMS) [10] .- For $K_L \rightarrow \gamma\gamma^*$ assumes the sequence $K_L \rightarrow K^*\gamma$; $K^* \rightarrow \rho, \omega, \phi$; $\rho, \omega, \phi \rightarrow \gamma^*$ where the weak $K^* \rightarrow \rho, \omega, \phi$ transition is computed using vacuum insertion. In the BMS model it is also assumed that the weak couplings in the non-leptonic weak four-quark hamiltonian are given by the perturbative Wilson coefficients with $\mathcal{O}(\alpha_s)$ corrections (i.e. there is no enhancement of $\Delta I = 1/2$ transitions in the weak vector–vector transitions). This model gives good results for $K_L \rightarrow \gamma\gamma^*$ but we will show that any reasonable value of the Wilson coefficients produces a too small result for the vector meson contribution to $K_L \rightarrow \pi^0\gamma\gamma$.

Actually the experimental determination of the slope in $K_L \rightarrow \gamma\gamma^*$ is only based in the BMS model. We analyse critically this experimental result and propose an alternative analysis less model dependent.

We realize also that the common problematic point between $K \rightarrow \pi\gamma\gamma$ and $K_L \rightarrow \gamma\gamma^*$ is the model dependence in the construction of the weak $VP\gamma$ vertex. Thus we have constructed the most general χ PT lagrangian for the weak $VP\gamma$ vertex for the processes under consideration. As we will show this gives us a quantitative relation between the two relevant parameters in $K \rightarrow \pi\gamma\gamma$ and $K_L \rightarrow \gamma\gamma^*$, thus correlating both processes.

Furthermore we propose a Factorization Model in the Vector couplings (FMV) that has as main ingredients :

- a) The application of the FM to the construction of the weak $VP\gamma$ vertex instead of the effective $K\pi\gamma\gamma$ and $K\gamma\gamma^*$ vertices as in the usual approach.
- b) We consider that the effective coupling of the FMV model (the only free parameter) is given by the Wilson coefficient in the non-leptonic hamiltonian.

We confront this model with the phenomenology and with the aforementioned models, particularly with the FM. Also we do a comparison with Ko's reference [21] where similar questions have been addressed.

The structure of the paper is as follows. In Section 2 we review briefly the treatment of non-leptonic weak interactions at low energy. In Section 3 we specify the kinematics and notation for our processes of interest. In Section 4 we propose our general framework. We construct the most general chiral structure of the octet piece for the weak $VP\gamma$ vertex. We also collect the lagrangian densities we will need in our study and we specify our conventions. Sections 5,6 and 7 are dedicated to review and discuss the predictions of the WDM, FM and BMS models for the observables in $K \rightarrow \pi\gamma\gamma$ and $K_L \rightarrow \gamma\gamma^*$. In Section 8 we propose our model in order to do a more complete evaluation of the factorizable contributions to the amplitudes. Results and conclusions of our work will be discussed in Sections 9 and 10 respectively.

2 Non-leptonic weak interactions at low energies

We will review in this Section the procedures of χ PT and their implementation in the study of non-leptonic weak processes. At the same time we will introduce our notations and the tools we will need in the development of our study.

2.1 Chiral Perturbation Theory

χ PT [1, 2] is an effective quantum field theory for the study of low energy strong interacting processes that relies in the exact chiral symmetry of massless QCD. Let $Z_{QCD}[v, a, s, p]$ be the generating functional of the QCD Green functions for the vector, axial, scalar and pseudoscalar quark currents,

$$e^{iZ_{QCD}[v, a, s, p]} = \int [DG_\mu] [Dq] [D\bar{q}] \exp \left\{ i \int d^4x \mathcal{L}_{QCD}[q, \bar{q}, G_\mu, v, a, s, p] \right\} , \quad (1)$$

$$\mathcal{L}_{QCD}[q, \bar{q}, G_\mu, v, a, s, p] = \mathcal{L}_{QCD}^0 + \bar{q} [\gamma_\mu (v^\mu + \gamma_5 a^\mu) - (s - i p \gamma_5)] q ,$$

where v^μ, a^μ, s and p are hermitian, colour neutral matrices in the flavour space representing the vector, axial, scalar and pseudoscalar external fields, respectively, and \mathcal{L}_{QCD}^0 is the QCD lagrangian density of three massless flavours and therefore is invariant under the chiral group $G \equiv SU(3)_L \otimes SU(3)_R$. In Eq. (1) q and G_μ are the quark and gluon fields respectively. The basic assumption of χ PT is that, at low energies ($E \leq 1 \text{ GeV}$), the chiral symmetry is spontaneously broken to the vector subgroup $SU(3)_V$,

$$SU(3)_L \otimes SU(3)_R \longrightarrow SU(3)_V ,$$

and then the generating functional admits a representation

$$e^{iZ_{QCD}[v,a,s,p]}|_{E \leq 1 \text{ GeV}} = \int [DU] \exp \left\{ i \int d^4x \mathcal{L}_{eff}(U, v, a, s, p) \right\} \quad , \quad (2)$$

where $U(\varphi)$ is a realization of the Goldstone bosons φ_i associated to the spontaneous breaking of the chiral symmetry and that are identified with the lightest hadronic spectra: the octet of pseudoscalar mesons. The unitary matrix $U(\varphi)$ transforms under the chiral group G as

$$U(\varphi) \xrightarrow{G} g_R U(\varphi) g_L^\dagger \quad , \quad (g_L, g_R) \in G \quad . \quad (3)$$

A convenient parameterization is given by

$$U(\varphi) = \exp \left(\frac{i}{F} \sum_{j=1}^8 \lambda_j \varphi_j \right) \quad , \quad (4)$$

where λ_i are the $SU(3)$ Gell-Mann matrices¹ and $F \sim F_\pi \simeq 93 \text{ MeV}$ is the decay constant of the pion.

Following the basic references by Callan, Coleman, Wess and Zumino [22] a more basic quantity $u(\varphi)$ is introduced. $u(\varphi)$ is an element of the coset space G/H , with $H = SU(3)_V$, that transforms under the chiral group as

$$u(\varphi) \xrightarrow{G} g_R u(\varphi) h(g, \varphi)^\dagger = h(g, \varphi) u(\varphi) g_L^\dagger \quad , \quad (5)$$

where the compensator field $h(g, \varphi) \in H$ is introduced. The relation between $U(\varphi)$ and $u(\varphi)$ is simple : $U = uu$.

The extension of the global chiral symmetry to a local one and the inclusion of external fields are convenient tools in order to work out systematically the Green functions of interest and the construction of chiral operators in the presence of symmetry breaking terms. A covariant derivative on the $U(\varphi)$ field is then defined as

$$D_\mu U = \partial_\mu U - i r_\mu U + i U \ell_\mu \quad , \quad (6)$$

where $\ell_\mu = v_\mu - a_\mu$ and $r_\mu = v_\mu + a_\mu$, in terms of the external vector and axial fields, are the left and right external fields, respectively. If only the electromagnetic field is considered (as we will do) then $\ell_\mu = r_\mu = -e Q A_\mu$ where $Q \equiv \text{diag}(2/3, -1/3, -1/3)$ is the electric charge matrix of the u, d and s quarks². The explicit symmetry breaking of the chiral symmetry due to the masses of the octet of pseudoscalars is included through the external scalar field $s = \mathcal{M} + \dots$

In this way the effective lagrangian in Eq. (2) can be constructed as an expansion in the external momenta (derivatives of the Goldstone fields) and masses as [1, 2, 3]

$$\mathcal{L}_{eff}(U, \ell, r, s, p) = \sum_n \mathcal{L}_{2n}(U, D_\mu U, \ell, r, s, p) \quad , \quad (7)$$

¹Normalized to $\text{Tr}(\lambda_i \lambda_j) = 2\delta_{ij}$.

²This corresponds to $D_\mu \phi^\pm = (\partial_\mu \pm ie A_\mu) \phi^\pm$.

(parity conservation requires an even number of derivatives). The leading $\mathcal{O}(p^2)$ strong lagrangian is

$$\mathcal{L}_2 = \frac{F^2}{4} \langle u_\mu u^\mu + \chi_+ \rangle , \quad (8)$$

where

$$\begin{aligned} u_\mu &\equiv i u^\dagger D_\mu U u^\dagger , & u_\mu &\xrightarrow{G} h(g, \varphi) u_\mu h(g, \varphi)^\dagger , \\ \chi_+ &\equiv u^\dagger \chi u^\dagger + u \chi^\dagger u & , & \chi \equiv 2 B_\circ (s + i p) \simeq 2 B_\circ \mathcal{M} + \dots , \\ \mathcal{M} &\equiv \text{diag}(m_u, m_d, m_s) & , & B_\circ \equiv -\frac{1}{F^2} \langle 0 | \bar{u} u | 0 \rangle , \end{aligned} \quad (9)$$

and $\langle A \rangle \equiv \text{Tr}(A)$ in the flavour space.

Starting at $\mathcal{O}(p^4)$ the strong chiral lagrangian has two well differentiated components corresponding to the vertices generating even- and odd-intrinsic parity transitions. The even-intrinsic parity lagrangian at $\mathcal{O}(p^4)$ was developed in [2] and introduces 12 unknown coupling constants. We will not use it in our study.

The $\mathcal{O}(p^4)$ odd-intrinsic parity lagrangian arises as a solution to the Ward condition imposed by the chiral anomaly [23]. The chiral anomalous functional $Z_{an}[U, \ell, r]$ as given by the Wess–Zumino–Witten action (WZW) is

$$\begin{aligned} Z_{an}[U, \ell, r]_{WZW} &= -\frac{iN_c}{240\pi^2} \int_{M^5} d^5x \epsilon^{ijklm} \langle \Sigma_i^L \Sigma_j^L \Sigma_k^L \Sigma_l^L \Sigma_m^L \rangle \\ &\quad - \frac{iN_c}{48\pi^2} \int d^4x \varepsilon_{\mu\nu\alpha\beta} (W(U, \ell, r)^{\mu\nu\alpha\beta} - W(I, \ell, r)^{\mu\nu\alpha\beta}) , \end{aligned} \quad (10)$$

$$\begin{aligned} W(U, \ell, r)_{\mu\nu\alpha\beta} &= \langle U \ell_\mu \ell_\nu \ell_\alpha U^\dagger r_\beta + \frac{1}{4} U \ell_\mu U^\dagger r_\nu U \ell_\alpha U^\dagger r_\beta + i U \partial_\mu \ell_\nu \ell_\alpha U^\dagger r_\beta \\ &\quad + i \partial_\mu r_\nu U \ell_\alpha U^\dagger r_\beta - i \Sigma_\mu^L \ell_\nu U^\dagger r_\alpha U \ell_\beta + \Sigma_\mu^L U^\dagger \partial_\nu r_\alpha U \ell_\beta \\ &\quad - \Sigma_\mu^L \Sigma_\nu^L U^\dagger r_\alpha U \ell_\beta + \Sigma_\mu^L \ell_\nu \partial_\alpha \ell_\beta + \Sigma_\mu^L \partial_\nu \ell_\alpha \ell_\beta \\ &\quad - i \Sigma_\mu^L \ell_\nu \ell_\alpha \ell_\beta + \frac{1}{2} \Sigma_\mu^L \ell_\nu \Sigma_\alpha^L \ell_\beta - i \Sigma_\mu^L \Sigma_\nu^L \Sigma_\alpha^L \ell_\beta \rangle \\ &\quad - (L \leftrightarrow R) , \end{aligned} \quad (11)$$

with

$$\begin{aligned} N_c &= 3 , \\ \Sigma_\mu^L &= U^\dagger \partial_\mu U , & \Sigma_\mu^R &= U \partial_\mu U^\dagger , \end{aligned}$$

and $(L \leftrightarrow R)$ stands for the interchange

$$U \leftrightarrow U^\dagger , \quad \ell_\mu \leftrightarrow r_\mu , \quad \Sigma_\mu^L \leftrightarrow \Sigma_\mu^R . \quad (12)$$

We see that the WZW action does not introduce any unknown coupling.

The $\mathcal{O}(p^6)$ strong lagrangian has recently been worked out in both even- and odd-intrinsic parity sectors [24].

It has to be observed that the presence of imaginary amplitudes as required by unitarity arises naturally in the perturbative expansion through loop computations at fixed chiral order which possible divergent parts are absorbed in the effective couplings of the chiral operators (as guaranteed by chiral symmetry [1]).

The inclusion of other quantum fields than the pseudoscalar Goldstone bosons in the chiral lagrangian was also considered in [22]. We are interested in the introduction of vector mesons coupled to the $U(\varphi)$ and the external fields. Let us then introduce the nonet of vector fields

$$V_\mu = \frac{1}{\sqrt{2}} \sum_{i=1}^8 \lambda_i V_\mu^i + \frac{1}{\sqrt{3}} V_\mu^0 \quad , \quad (13)$$

that transforms homogeneously under the chiral group as

$$V_\mu \xrightarrow{G} h(g, \varphi) V_\mu h(g, \varphi)^\dagger \quad (14)$$

and ideal mixing, i.e. $V_8^\mu = (\omega^\mu + \sqrt{2} \phi^\mu) / \sqrt{3}$, is assumed.

The most general strong vector-pseudoscalar-photon ($VP\gamma$) vertex, assuming nonet symmetry, at leading $\mathcal{O}(p^3)$ reads [18]

$$\mathcal{L}(VP\gamma) = h_V \varepsilon_{\mu\nu\rho\sigma} \langle V^\mu \{ u^\nu, f_+^{\rho\sigma} \} \rangle \quad , \quad (15)$$

where

$$f_+^{\mu\nu} = u F_L^{\mu\nu} u^\dagger + u^\dagger F_R^{\mu\nu} u \quad , \quad f_+^{\mu\nu} \xrightarrow{G} h(g, \varphi) f_+^{\mu\nu} h(g, \varphi)^\dagger \quad , \quad (16)$$

and $F_{R,L}^{\mu\nu}$ are the strength field tensors associated to the external r_μ and ℓ_μ fields. In Eq. (15), from the experimental width $\Gamma(\omega \rightarrow \pi^0 \gamma)$ [25], $|h_V| = (3.7 \pm 0.3) \times 10^{-2}$.

The most general vector-photon ($V\gamma$) coupling, at leading $\mathcal{O}(p^3)$, can be written as

$$\mathcal{L}(V\gamma) = -\frac{f_V}{2\sqrt{2}} \langle V_{\mu\nu} f_+^{\mu\nu} \rangle \quad , \quad (17)$$

where $V_{\mu\nu} = \nabla_\mu V_\nu - \nabla_\nu V_\mu$ and ∇_μ is the covariant derivative defined in [4] as

$$\nabla_\mu A = \partial_\mu A + [\Gamma_\mu, A] \quad (18)$$

$$\Gamma_\mu \equiv \frac{1}{2} \left\{ u^\dagger (\partial_\mu - i r_\mu) u + u (\partial_\mu - i \ell_\mu) u^\dagger \right\}$$

for any A operator that transforms homogeneously as the vector field in Eq. (14). In Eq. (17), $|f_V| \simeq 0.20$ as obtained from the experimental width $\Gamma(\rho^0 \rightarrow e^+ e^-)$ [25]. Moreover the positive slope of the $\pi^0 \rightarrow \gamma \gamma^*$ form factor determined experimentally tells us that the effective couplings in Eqs. (15, 17) must satisfy $h_V f_V > 0$.

It has to be noted that the incorporation of vector mesons in chiral lagrangians is not unique and several realizations of the vector field can be employed. In particular the antisymmetric formulation of vector fields was seen to implement automatically vector meson dominance at $\mathcal{O}(p^4)$ in χ PT [4]. In [26] was shown that, at $\mathcal{O}(p^4)$ in χ PT, once high energy QCD constraints are taken into account, the usual realizations (antisymmetric, vector, Yang–Mills and Hidden formulations) are equivalent. Although the antisymmetric tensor formulation of spin–1 mesons was proven to have a better high–energy behaviour than the vector field realization at $\mathcal{O}(p^4)$, this fact is not necessarily the case in general. In fact for the odd–intrinsic parity coupling relevant in $V \rightarrow P\gamma$ decays, the antisymmetric tensor formulation only contributes at $\mathcal{O}(p^8)$ while QCD requires explicit $\mathcal{O}(p^6)$ terms [18]. This is the reason why we will use the vector field formulation (already introduced in Eqs. (15,17)) that provides the right behaviour in the processes of our interest. We will also see that the hidden gauge formalism [27] provides also the straightforward $\mathcal{O}(p^6)$ operators.

For a further extensive and thorough exposition on χ PT see [28, 29, 30].

2.2 Non–leptonic weak interactions in χ PT

At low energies ($E \ll M_W$) the $\Delta S = 1$ effective weak hamiltonian (where only the degrees of freedom of the light quark fields remain) is obtained from the Lagrangian of the Standard Model by using the asymptotic freedom property of QCD in order to integrate out the fields with heavy masses down to scales $\mu < m_c$. It reads

$$\mathcal{H}_{NL}^{|\Delta S|=1} = -\frac{G_F}{\sqrt{2}} V_{ud}V_{us}^* \sum_{i=1}^6 C_i(\mu) Q_i + h.c. \quad . \quad (19)$$

Here G_F is the Fermi constant, V_{ij} are elements of the CKM-matrix, $C_i(\mu)$ are the Wilson coefficients of the four–quark operators Q_i , $i = 1, \dots, 6$. In Eq. (19) only 6 operators appear if no virtual electromagnetic interactions nor leptons are included [7, 31, 32]. In the following we only will be interested on Q_1 and Q_2 and not on the Q_3, \dots, Q_6 QCD penguin operators [33].

If we neglect QCD corrections Eq. (19) reduces to

$$\begin{aligned} \mathcal{H}_{NL}^{|\Delta S|=1} &= -\frac{G_F}{\sqrt{2}} V_{ud}V_{us}^* Q_2 + h.c. \\ &= -\frac{G_F}{\sqrt{2}} V_{ud}V_{us}^* 4 (\bar{s}_L \gamma^\mu u_L)(\bar{u}_L \gamma_\mu d_L) + h.c. \quad , \end{aligned} \quad (20)$$

with $\bar{s}_L \gamma_\mu u_L \equiv \frac{1}{2} \bar{s}^\alpha \gamma_\mu (1 - \gamma_5) u_\alpha$, and α a colour index.

If the effect of gluon exchange at leading order is considered, the operator Q_2 in Eq. (20) is not multiplicatively renormalizable but mixes with a new operator [34, 35]

$$Q_1 \equiv 4 (\bar{s}_L \gamma^\mu d_L)(\bar{u}_L \gamma_\mu u_L) \quad . \quad (21)$$

Then we can consider the linear combinations

$$Q_{\pm} = Q_2 \pm Q_1 \quad , \quad (22)$$

that do not mix under renormalization. We can write therefore

$$\mathcal{H}_{NL}^{|\Delta S|=1} = -\frac{G_F}{2\sqrt{2}} V_{ud} V_{us}^* [C_+(\mu) Q_+ + C_-(\mu) Q_-] + h.c. \quad . \quad (23)$$

Considering the isospin quantum numbers $Q_+ \sim \Delta I = 3/2$ and $Q_- \sim \Delta I = 1/2$. Already the leading order computation of the Wilson coefficients shows that the C_+ coefficient is suppressed and the C_- enhanced indicating the right direction addressed by the phenomenology. However quantitatively the enhancement is not big enough. In our further discussion we will ignore the Q_+ operator, that is, we will not take into account the $\Delta I = 3/2$ transitions.

In our study we consider the leading $\mathcal{O}(\alpha_s)$ order Wilson coefficients [34, 35]. We choose the hadronic scale $\mu = m_\rho$ and $\Lambda_{\overline{MS}} = (325 \pm 110) \text{ MeV}$. This gives

$$C_-(m_\rho) = 2.2_{-0.2}^{+0.5} \quad , \quad (24)$$

where the error only includes the incertitude in $\Lambda_{\overline{MS}}$ ³. For our further discussion let us introduce the parameters G_8^{sd} and g_8^{sd} defined by

$$\mathcal{H}_{NL}^{|\Delta S|=1} \equiv -G_8^{sd} Q_- + h.c. \equiv -\frac{G_F}{\sqrt{2}} V_{ud} V_{us}^* g_8^{sd} Q_- + h.c. \quad , \quad (25)$$

where the superscript “sd” is short for “short-distance”. The Q_- operator admits a realization in χ PT. The hamiltonian in Eq. (25) behaves under $SU(3)_L \otimes SU(3)_R$ as

$$\mathcal{H}_{NL}^{|\Delta S|=1} \sim (8_L, 1_R) \quad . \quad (26)$$

Then at $\mathcal{O}(p^2)$, leading order in χ PT, we can construct an effective lagrangian using the left-handed currents associated to the chiral transformations,

$$\begin{aligned} \mathcal{L}_2^{|\Delta S|=1} &= 4 G_8 \langle \lambda_6 L_1^\mu L_\mu^1 \rangle \\ &= G_8 F^4 \langle \Delta u_\mu u^\mu \rangle \quad , \end{aligned} \quad (27)$$

where

$$L_\mu^1 = \frac{\delta S_2^x}{\delta \ell^\mu} = -i \frac{F^2}{2} U^\dagger D_\mu U = -\frac{F^2}{2} u^\dagger u_\mu u \quad , \quad (28)$$

³The Wilson coefficients have recently been computed at next-to-leading order by two teams and using two regularization procedures [31, 32] with compatible results. At next-to-leading order the Q_- operator mixes with the penguin operators Q_i , $i = 3, 4, 5, 6$. As we are not considering these contributions we use the leading order Wilson coefficients.

is the left-handed current associated to the S_2^χ action of the $\mathcal{O}(p^2)$ strong lagrangian Eq. (8) and $\Delta = u \lambda_6 u^\dagger$. The bosonization represented by $\mathcal{L}_2^{|\Delta S|=1}$ of the Q_- operator amounts to the assumption of factorization of the four-quark operator as we will explain later.

Now let us discuss the value of the effective coupling G_8 or, alternatively, g_8 . From the experimental width of $K \rightarrow \pi\pi$ and the use of $\mathcal{L}_2^{|\Delta S|=1}$ Eq. (27), that is, at $\mathcal{O}(p^2)$ one gets ⁴

$$|g_8|_{K \rightarrow \pi\pi} \simeq 5.1 \quad , \quad |G_8|_{K \rightarrow \pi\pi} \equiv |G_8| \simeq 9.2 \times 10^{-6} \text{ GeV}^{-2} \quad . \quad (29)$$

If instead of defining the g_8 coupling as in Eq. (25) we had used the leading $1/N_c$ operator Q_2 , the evaluation of the matrix element in $K \rightarrow \pi\pi$ using factorization at leading order would have had predicted $g_8^{K \rightarrow \pi\pi} = 3/5$, showing that the leading $1/N_c$ operator Q_2 is not able of implementing the $\Delta I = 1/2$ enhancement in $K \rightarrow \pi\pi$ transitions as it is well known. If instead we use the result for the Wilson coefficient $C_-(m_\rho)$ Eq. (24) we see that

$$g_8^{sd}|_{Wilson} = \frac{1}{2} C_-(m_\rho) \simeq 1.1 \quad , \quad (30)$$

showing, as commented before, and enhancement of the $1/N_c$ result but still far away from the phenomenological value in Eq. (29). Of course it has to be taken into account that we are ignoring the short-distance contribution of the penguin operators Q_i , $i = 3, 4, 5, 6$ in Eq. (19) that also enhances the $\Delta I = 1/2$ transitions.

At $\mathcal{O}(p^4)$ the chiral weak lagrangian has been studied in [37, 38] giving 48 chiral operators W_i only in the octet part

$$\mathcal{L}_4^{|\Delta S|=1} = G_8 F^2 \sum_{i=1}^{48} N_i W_i + h.c. \quad , \quad (31)$$

that gives 48 new unknown coupling constants N_i . Their phenomenological determination is then very difficult and models are necessary in order to predict them [38, 39]. We will briefly review the two more popular and successful :

a) Factorization Model

The Factorization Model (FM) [20, 38, 40] assumes that the dominant contribution of the four-quark operators of the $\Delta S = 1$ Hamiltonian comes from a factorization *current* \times *current* of them. This assumption is implemented with a bosonization of the left-handed quark currents in χ PT as given by

$$\overline{q_{jL}} \gamma^\mu q_{iL} \longleftrightarrow \frac{\delta S[U, \ell, r, s, p]}{\delta \ell_{\mu, ji}} \quad , \quad (32)$$

where i, j are flavour indices, and $S[U, \ell, r, s, p]$ is the low-energy strong effective action of QCD in terms of the Goldstone bosons realization U and the external fields ℓ, r, s, p .

⁴If $\mathcal{O}(p^4)$ corrections are taken into account, a phenomenological value of $|g_8| \simeq 3.6$ is obtained [36].

The general form of the lagrangian (assuming traceless left-handed currents) is

$$\mathcal{L}_{FM} = 4 k_F G_8 \langle \lambda \frac{\delta S}{\delta \ell_\mu} \frac{\delta S}{\delta \ell^\mu} \rangle + h.c. \quad , \quad (33)$$

where $\lambda \equiv \frac{1}{2}(\lambda_6 - i\lambda_7)$ and

$$\frac{\delta S}{\delta \ell^\mu} \equiv L_\mu = L_\mu^1 + L_\mu^3 + L_\mu^5 + \dots \quad (34)$$

the left-handed current which first term L_μ^1 was already given in Eq. (28). The FM gives a full prediction but for a fudge factor k_F that is not given by the model. $k_F = 1$ in the naive factorization approach (nFM) and in general $k_F \sim \mathcal{O}(1)$. The nFM ($k_F = 1$) would correspond to inputting the $\Delta I = 1/2$ enhancement once the left-handed currents are generated by the full relevant strong lagrangian. Thus caution is needed in order to interpret this factor.

b) Weak Deformation Model

The WDM [18, 19] assumes that the dominant effect at long distances of the left-handed $\Delta S = 1$ Lagrangian can be obtained through a deformation of the two 1-forms defined in the coset space of the spontaneously broken chiral group. The deformation is defined in such a way that leaves the right-chiral 1-form unchanged and only affects to the left-chiral 1-form. A characteristic feature of the model is that gives predictions for the weak couplings in terms of the strong coupling constants (in a scale independent manner). Even when the dynamics behind the WDM is not clear its phenomenological applications might be successful and in any case they deserve to be tested.

It has been shown in [38] that the WDM can be expressed through the lagrangian

$$\mathcal{L}_{WDM} = 2 G_8 \langle \lambda \left\{ L_\mu^1, \frac{\delta S}{\delta \ell_\mu} \right\} \rangle + h.c. \quad , \quad (35)$$

and comparing with \mathcal{L}_{FM} in Eq. (33) one sees that, at $\mathcal{O}(p^4)$, $\mathcal{L}_{WDM} = \mathcal{L}_{FM}(k_F = 1/2)$, but at higher chiral orders the FM can have additional terms. The equivalence between WDM and FM for $k_F = 1/2$ has been proven in general at $\mathcal{O}(p^4)$ in χ PT [38]. However this equivalence can be extended at $\mathcal{O}(p^6)$ ⁵ if the lagrangian is still a product of currents $\mathcal{O}(p)$ and $\mathcal{O}(p^5)$.

3 $K \rightarrow \pi \gamma \gamma$ and $K_L \rightarrow \gamma \gamma^*$ amplitudes

The general amplitude for $K \rightarrow \pi \gamma \gamma$ is given by

$$M(K(p) \rightarrow \pi \gamma(q_1, \epsilon_1) \gamma(q_2, \epsilon_2)) = \epsilon_{1\mu} \epsilon_{2\nu} M^{\mu\nu}(p, q_1, q_2) \quad , \quad (36)$$

⁵G. Ecker, private communication.

where ϵ_1, ϵ_2 are the photon polarizations, and $M^{\mu\nu}$ has four invariant amplitudes [41]

$$\begin{aligned}
M^{\mu\nu} = & \frac{A(z, y)}{m_K^2} (q_2^\mu q_1^\nu - q_1 \cdot q_2 g^{\mu\nu}) + \frac{2 B(z, y)}{m_K^4} (-p \cdot q_1 p \cdot q_2 g^{\mu\nu} - q_1 \cdot q_2 p^\mu p^\nu \\
& + p \cdot q_1 q_2^\mu p^\nu + p \cdot q_2 p^\mu q_1^\nu) \\
& + \frac{C(z, y)}{m_K^2} \varepsilon^{\mu\nu\rho\sigma} q_{1\rho} q_{2\sigma} + \frac{D(z, y)}{m_K^4} [\varepsilon^{\mu\nu\rho\sigma} (p \cdot q_2 q_{1\rho} + p \cdot q_1 q_{2\rho}) p_\sigma \\
& + (p^\mu \varepsilon^{\nu\alpha\beta\gamma} + p^\nu \varepsilon^{\mu\alpha\beta\gamma}) p_\alpha q_{1\beta} q_{2\gamma}]
\end{aligned} \tag{37}$$

and

$$y = \frac{p \cdot (q_1 - q_2)}{m_K^2}, \quad z = \frac{(q_1 + q_2)^2}{m_K^2}. \tag{38}$$

The physical region in the adimensional variables y and z is given by :

$$0 \leq |y| \leq \frac{1}{2} \lambda^{1/2}(1, r_\pi^2, z), \quad 0 \leq z \leq (1 - r_\pi)^2, \tag{39}$$

with

$$\begin{aligned}
\lambda(a, b, c) &= a^2 + b^2 + c^2 - 2(ab + ac + bc), \\
r_\pi &= \frac{m_\pi}{m_K}.
\end{aligned} \tag{40}$$

Note that the invariant amplitudes $A(z, y)$, $B(z, y)$ and $C(z, y)$ have to be symmetric under the interchange of q_1 and q_2 as required by Bose symmetry, while $D(z, y)$ is anti-symmetric. In the limit where CP is conserved the amplitudes A and B contribute only to $K_L \rightarrow \pi^0 \gamma \gamma$ while C and D only contribute to $K_S \rightarrow \pi^0 \gamma \gamma$. In $K^+ \rightarrow \pi^+ \gamma \gamma$ all of them are involved.

Using the definitions Eqs. (37,38) the double differential rate for unpolarized photons is given by

$$\begin{aligned}
\frac{\partial^2 \Gamma}{\partial y \partial z} = & \frac{m_K}{2^9 \pi^3} \left[z^2 (|A + B|^2 + |C|^2) \right. \\
& \left. + \left(y^2 - \frac{1}{4} \lambda(1, r_\pi^2, z) \right)^2 (|B|^2 + |D|^2) \right].
\end{aligned} \tag{41}$$

The processes $K \rightarrow \pi \gamma \gamma$ have no tree level $\mathcal{O}(p^2)$ contribution because there are not enough powers of momenta to satisfy the constraint of gauge invariance. For this same reason at $\mathcal{O}(p^4)$ the amplitudes B and D are still zero. Therefore their leading contribution is $\mathcal{O}(p^6)$. As can be seen from Eq. (41) only the B and D terms contribute for small z (the invariant amplitudes are regular in the small y, z region). The antisymmetric character of the D amplitude under the interchange of q_1 and q_2 means effectively that while its

leading contribution is $\mathcal{O}(p^6)$ this only can come from a finite loop calculation because the leading counterterms for the D amplitude are $\mathcal{O}(p^8)$ ⁶. However also this loop contribution is helicity suppressed compared to the B term. As shown in a similar situation in the electric Direct Emission of $K_L \rightarrow \pi^+\pi^-\gamma$ [42] this antisymmetric $\mathcal{O}(p^6)$ loop contribution might be smaller than the local $\mathcal{O}(p^8)$ contribution.

Thus in the region of small z (collinear photons) the B amplitude is dominant and can be determined separately from the A amplitude. This feature is important in order to evaluate the CP conserving contribution $K_L \rightarrow \pi^0\gamma\gamma \rightarrow \pi^0e^+e^-$. Both on-shell and off-shell two-photon intermediate states generate, through the A amplitude, a contribution to $K_L \rightarrow \pi^0e^+e^-$ that is proportional to m_e/m_K and therefore suppressed [41]. Otherwise the B -type amplitude, though appearing only at $\mathcal{O}(p^6)$, generates a relevant unsuppressed contribution to $K_L \rightarrow \pi^0e^+e^-$ through the on-shell photons [11, 12, 13], due to the different helicity structure. The dispersive two-photon contribution generated by the B -type amplitude has been approximated by choosing an appropriate form factor for the virtual photon coupling [43].

The amplitude for $K_L \rightarrow \gamma\gamma^*$ (neglecting any CP-violating effects) is given by

$$M(K_L(p) \rightarrow \gamma(q_1, \epsilon_1)\gamma^*(q_2, \epsilon_2)) = i A_{\gamma\gamma^*}(q_2^2) \varepsilon_{\mu\nu\sigma\tau} \epsilon_1^\mu(q_1) \epsilon_2^\nu(q_2) q_1^\sigma q_2^\tau, \quad (42)$$

The unique amplitude $A_{\gamma\gamma^*}(q_2^2)$ we can express as

$$A_{\gamma\gamma^*}(q_2^2) = A_{\gamma\gamma}^{exp} f(x), \quad (43)$$

where $A_{\gamma\gamma}^{exp}$ is the experimental amplitude $A(K_L \rightarrow \gamma\gamma)$ and $x = q_2^2/m_K^2$. The form factor $f(x)$ in Eq. (43) is properly normalized to $f(0) = 1$. We define the slope b of $f(x)$ as

$$f(x) = 1 + bx + \mathcal{O}(x^2). \quad (44)$$

The differential decay spectrum for $K_L \rightarrow \gamma\ell^+\ell^-$, in the absence of radiative corrections, is given by

$$\frac{1}{\Gamma_{\gamma\gamma}} \frac{d\Gamma}{dx} = \frac{2\alpha}{3\pi} \frac{(1-x)^3}{x} \left(1 + \frac{2m_\ell^2}{xm_K^2} \right) \sqrt{1 - \frac{4m_\ell^2}{xm_K^2}} |f(x)|^2, \quad (45)$$

where $\Gamma_{\gamma\gamma}$ is the $K_L \rightarrow \gamma\gamma$ decay rate.

4 Local contributions to $K \rightarrow \pi\gamma\gamma$ and $K_L \rightarrow \gamma\ell^+\ell^-$ generated by vector resonance exchange : general framework

The leading finite $\mathcal{O}(p^4)$ amplitudes of $K_L \rightarrow \pi^0\gamma\gamma$ were evaluated some time ago [44], generating only the A -type amplitude in Eq. (37). No local contributions arise since all

⁶This is so due to the fact that its antisymmetric property demands that its leading contribution cannot be a constant term.

the external particles involved are electrically neutral. Thus the loop amplitude is simply predicted in terms of G_8 from $\mathcal{O}(p^2)$ $K \rightarrow \pi\pi$ Eq. (29) (and the corresponding G_{27} when $\Delta I = 3/2$ transitions are taken into account [14]).

Also the leading $\mathcal{O}(p^4)$ amplitudes for $K^+ \rightarrow \pi^+\gamma\gamma$ were computed in [41]. At this order both the A - and C -type amplitudes in Eq. (37) appear. The C amplitude is generated by the Wess–Zumino–Witten anomalous vertex $\pi^0 \rightarrow \gamma\gamma$ [23] and consequently is completely determined at leading $\mathcal{O}(p^4)$. Though the leading order is finite, chiral symmetry allows a scale independent local contribution to the A amplitude. The counterterm combination can be written in terms of strong and weak effective couplings as

$$\hat{c} = \frac{128\pi^2}{3} [3(L_9 + L_{10}) + N_{14} - N_{15} - 2N_{18}] \quad , \quad (46)$$

where L_9 and L_{10} are known couplings of the $\mathcal{O}(p^4)$ χ PT strong lagrangian [2] and N_i are couplings of the $\mathcal{O}(p^4)$ weak χ PT lagrangian Eq. (31) [37, 38]. Since weak counterterms are involved in Eq. (46), resonance exchange is not sufficient to make predictions and models have to be invoked [38, 39, 45]. Interestingly enough, the combination of weak couplings in Eq. (46) is an independent relation to take into account in order to determine the $\mathcal{O}(p^4)$ weak couplings [6] and to test the models.

The observed branching ratio for $K_L \rightarrow \pi^0\gamma\gamma$ is

$$Br(K_L \rightarrow \pi^0\gamma\gamma)|_{exp} = (1.7 \pm 0.3) \times 10^{-6} \quad [NA31, [46]] \quad , \quad (47)$$

$$Br(K_L \rightarrow \pi^0\gamma\gamma)|_{exp} = (1.86 \pm 0.60 \pm 0.60) \times 10^{-6} \quad [E731, [47]] \quad .$$

which is substantially larger than the $\mathcal{O}(p^4)$ prediction [44, 14]

$$Br(K_L \rightarrow \pi^0\gamma\gamma)|_{\mathbf{8+27}}^{\mathcal{O}(p^4)} \simeq 0.61 \times 10^{-6} \quad . \quad (48)$$

However the $\mathcal{O}(p^4)$ spectrum of the diphoton invariant mass nearly agrees with the experiment, in particular no events for small $m_{\gamma\gamma}$ are observed, implying a small B -type amplitude. Thus $\mathcal{O}(p^6)$ corrections have to be important. Though no complete calculation is available, the supposedly larger contributions have been performed : $\mathcal{O}(p^6)$ unitarity corrections from $K_L \rightarrow \pi^0\pi^+\pi^-$ were worked out in [14, 15], they enhance the $\mathcal{O}(p^4)$ branching ratio by 30%,

$$Br(K_L \rightarrow \pi^0\gamma\gamma)|_{unitarity}^{\mathcal{O}(p^6)} \simeq 0.84 \times 10^{-6} \quad , \quad (49)$$

and generate a B -type amplitude slightly spoiling the satisfactory $\mathcal{O}(p^4)$ spectrum.

$\mathcal{O}(p^6)$ loop contributions to $K \rightarrow \pi\gamma\gamma$ are in general divergent and need to be regularized. Lorentz and gauge invariance give four different local structures at $\mathcal{O}(p^6)$ for $K \rightarrow \pi\gamma\gamma$ processes :

$$F_{\mu\nu} F^{\mu\nu} \partial_\lambda K \partial^\lambda \pi \quad , \quad m_K^2 F_{\mu\nu} F^{\mu\nu} K \pi \quad ,$$

(50)

$$\partial^\alpha F_{\mu\nu} \partial_\alpha F^{\mu\nu} K^+ \pi^- \quad , \quad F_{\mu\nu} F^{\mu\lambda} \partial^\nu K \partial_\lambda \pi \quad .$$

Here both neutral and charged mesons are understood and the term with derivatives on the photon strength field tensor only appears for electrically charged mesons. It is necessary to emphasize that there is no reason why the effective couplings of these structures have to coincide in the neutral and charged channels because different chiral structures in both channels can give the local terms in Eq. (50). Between the different structures in Eq. (50) only the last one contributes to a B amplitude in Eq. (37).

The physics behind the couplings weighting the weak local amplitudes in Eq. (50) has not been fully investigated. The situation in weak χ PT is not as established as in the strong sector, a fact that was mentioned earlier, but it is sound to think that the lightest non-Goldstone meson spectrum plays a major role. In particular we will concentrate in the possible contribution of vector resonances and we disregard heavier states which contribution is expected to be smaller. In the generation of the structures in Eq. (50) we find that only the terms with derivatives on the meson fields can be generated by vector meson exchange.

In [18] two different vector generated amplitudes for $K \rightarrow \pi\gamma\gamma$ were considered : i) a strong vector exchange with a weak transition in a external leg (diagrams in Figs. 1.a and 1.b), and ii) a direct vector exchange between a weak $VP\gamma$ vertex and a strong one (diagrams in Figs. 1.c and 1.d). The BMS model [10] suggests a third direct contribution: iii) a weak vector-vector transition as in diagram of Fig. 1.e. While the first contribution is well under control from the phenomenology of strong interactions, the second case depends strongly on the model used for the weak $VP\gamma$ vertex. Presently two well known models have been used, the Weak Deformation Model (WDM) [18] and the Factorization Model (FM) [20, 38] which predictions we will review later on.

The diagram in Fig. 1.a was advocated to generate large local contributions to $K_L \rightarrow \pi^0\gamma\gamma$, such that, if added to the $\mathcal{O}(p^4)$ loop amplitude, could accomodate the disagreement in the width [12, 48]. However due to the presence of a local B -type amplitude, the spectrum, particularly at low $m_{\gamma\gamma}$, does not agree with experiment. Furthermore in some models (like WDM) [18] there is a tendency to a cancellation between diagrams in Figs. 1.a, 1.b and Figs. 1.c, 1.d. Nevertheless no definitive statement about the resonance exchange role has yet been made.

Cohen , Ecker and Pich noticed [15] that by adding the contributions from the diagrams in Figs. 1.a,1.b,1.c and 1.d, for a choice of the unknown weak coupling in diagrams Figs. 1.c and 1.d, one could, simultaneously, obtain the experimental spectrum and width of $K_L \rightarrow \pi^0\gamma\gamma$.

Finally, a Khuri-Treiman unitarization of the $K_L \rightarrow \pi^0\gamma\gamma$ through the $K \rightarrow \pi\pi\pi$

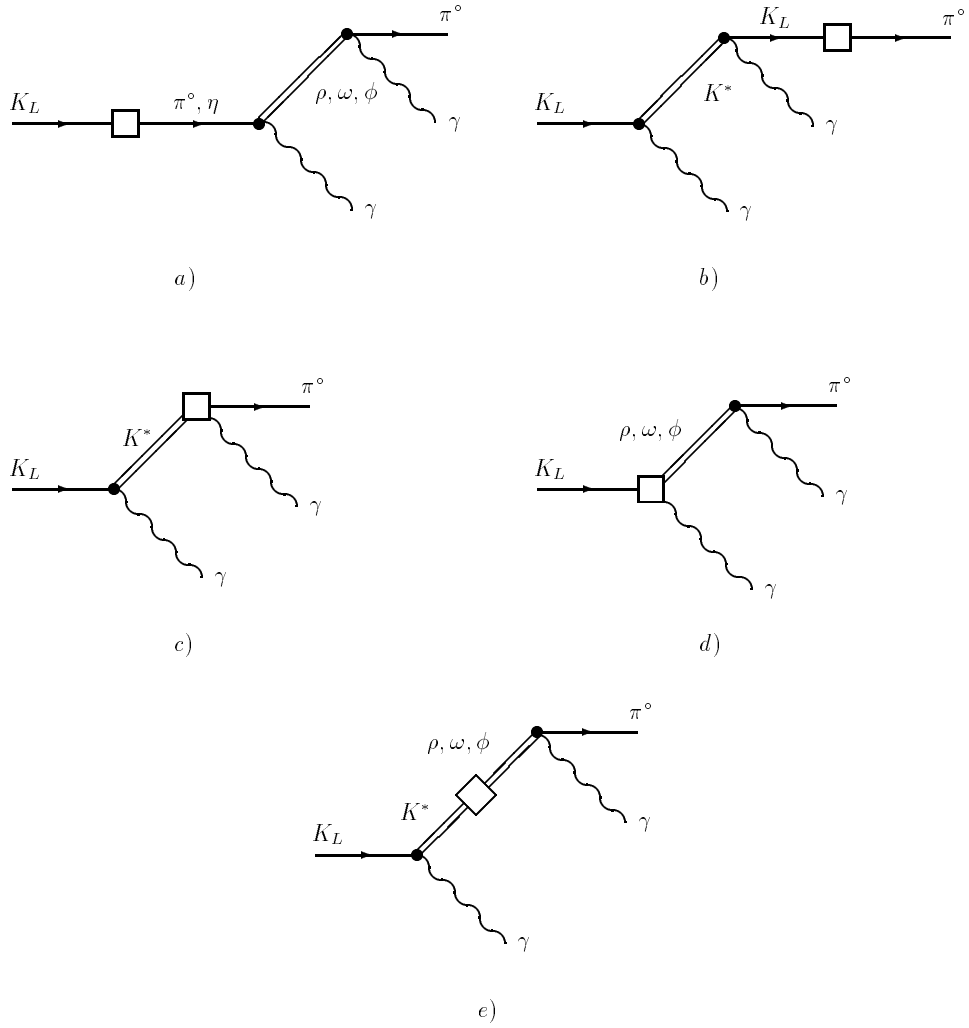


Figure 1: Feynman diagrams for $K_L \rightarrow \pi^0 \gamma \gamma$. a) and b) correspond to *external* weak transitions, c) and d) to *direct* weak transitions. e) is the contribution of the BMS model to the *direct* weak transitions. Analogous to these contribute to $K^+ \rightarrow \pi^+ \gamma \gamma$.

intermediate state [49]⁷, and the inclusion of the experimental $\gamma\gamma \rightarrow \pi^0\pi^0$ amplitude, increased the A amplitude by another 10%.

The $\mathcal{O}(p^6)$ unitarity corrections from $K^+ \rightarrow \pi^+\pi^+\pi^-$ to $K^+ \rightarrow \pi^+\gamma\gamma$ have been computed in [17] and found to produce a B -type amplitude. This contribution increases the rate by a 30–40%. Differently from $K_L \rightarrow \pi^0\gamma\gamma$, $\mathcal{O}(p^6)$ vector meson exchange seems to be negligible in $K^+ \rightarrow \pi^+\gamma\gamma$ [17], at least in the FM and WDM. It is worth stressing that the question of the size of $\mathcal{O}(p^6)$ vector meson exchange contribution can be studied independently from the A amplitude in the region of small diphoton invariant mass. Thus the value of \hat{c} in Eq. (46) can be studied in the remaining kinematical region. BNL-787 has got, for the first time [16], events in this channel and similarly KLOE at DAΦNE will do in the foreseen future.

Consequently the perspectives to a parallel analysis of $K_L \rightarrow \pi^0\gamma\gamma$ and $K^+ \rightarrow \pi^+\gamma\gamma$ are very good and therefore the questions of the size of vector meson exchange and the completeness of the computed $\mathcal{O}(p^6)$ contributions can be answered. The situation will be even better if we know more accurately the vector meson exchange contribution : in this paper we pursue the idea that a good weak vector meson model has to describe simultaneously the $\mathcal{O}(p^6)$ slope in $K_L \rightarrow \gamma\gamma^*$ and the $\mathcal{O}(p^6)$ vector meson contribution to $K_L \rightarrow \pi^0\gamma\gamma$; then, as a further prediction, to $K^+ \rightarrow \pi^+\gamma\gamma$.

Hence we can think of a general framework where we consider the full structure of the weak $VP\gamma$ vertex that belongs to the octet representation of $SU(3)_L$ ⁸. Then the most general effective weak coupling $VP\gamma$ able to contribute to $\mathcal{O}(p^6)$ $K \rightarrow \pi\gamma\gamma$ and $K_L \rightarrow \gamma\gamma^*$ processes is

$$\mathcal{L}_W(VP\gamma) = G_8 F_\pi^2 \langle V^\mu \mathcal{J}_\mu^W \rangle \quad , \quad (51)$$

where

$$\mathcal{J}_\mu^W = \varepsilon_{\mu\nu\alpha\beta} \sum_{i=1}^5 \kappa_i T_i^{\nu\alpha\beta} \quad , \quad (52)$$

and

$$\begin{aligned} T_1^{\nu\alpha\beta} &= \{ u^\nu, \Delta f_+^{\alpha\beta} \} \quad , \\ T_2^{\nu\alpha\beta} &= \{ \{ \Delta, u^\nu \}, f_+^{\alpha\beta} \} \quad , \\ T_3^{\nu\alpha\beta} &= \langle u^\nu \Delta \rangle f_+^{\alpha\beta} \quad , \\ T_4^{\nu\alpha\beta} &= \langle u^\nu f_+^{\alpha\beta} \rangle \Delta \quad , \\ T_5^{\nu\alpha\beta} &= \langle \Delta u^\nu f_+^{\alpha\beta} \rangle \quad . \end{aligned} \quad (53)$$

In Eq. (52) κ_i , $i = 1, 2, 3, 4, 5$ are dimensionless coupling constants to be determined from phenomenology or theoretical models. There are other terms for processes involving more

⁷In [49] only the dominant S-wave component in $\pi\pi$ scattering has been taken into account and therefore only an A -type amplitude is generated by these corrections.

⁸We will not consider operators of the **27** representation of $SU(3)_L$ because their contribution is presumably much less important.

pseudoscalars. We use, as anticipated in Section 2.1, the usual formulation of vector fields to describe the vector mesons.

4.1 $K \rightarrow \pi\gamma\gamma$

By integrating out the vector meson fields interchanged between one vertex from $\mathcal{L}_W(VP\gamma)$ Eq. (51) and a vertex from $\mathcal{L}(VP\gamma)$ Eq. (15) we generate a lagrangian that provides local $\mathcal{O}(p^6)$ contributions to $K \rightarrow \pi\gamma\gamma$. The result is

$$\begin{aligned} \mathcal{L}_6^W = & -\frac{128\pi}{9} G_8 \alpha_{em} \frac{h_V}{m_V^2} \left[F^{\mu\nu} F_{\mu\nu} \left[(2\kappa_1 + 4\kappa_2 - 3\kappa_3 + 3\kappa_4 + 3\kappa_5) \partial^\alpha K_2^0 \partial_\alpha \pi^0 \right. \right. \\ & \left. \left. + (\kappa_1 - \kappa_2) (\partial^\alpha K^+ \partial_\alpha \pi^- + \partial^\alpha K^- \partial_\alpha \pi^+) \right] \right. \\ & \left. + 2 F^{\mu\nu} F_{\nu\lambda} \left[(2\kappa_1 + 4\kappa_2 - 3\kappa_3 + 3\kappa_4 + 3\kappa_5) \partial^\lambda K_2^0 \partial_\mu \pi^0 \right. \right. \\ & \left. \left. + (\kappa_1 - \kappa_2) (\partial^\lambda K^+ \partial_\mu \pi^- + \partial^\lambda K^- \partial_\mu \pi^+) \right] \right] \quad , \end{aligned} \quad (54)$$

where m_V is the degenerate mass of the vector mesons in the chiral limit and $K_2^0 = K_L$ in the CP limit.

If we compare Eq. (54) with Eq. (50) we see that, as we already commented, only the terms with derivatives over the meson fields are generated by vector resonance exchange. \mathcal{L}_6^W generates A and B amplitudes in Eq. (37). Moreover Vector Meson Dominance and the restrictions of chiral symmetry show that the combination of weak structures in Eq. (52) to $F^{\mu\nu} F_{\mu\nu} \partial^\alpha K \partial_\alpha \pi$ and $F^{\mu\nu} F_{\nu\lambda} \partial^\lambda K \partial_\mu \pi$ in Eq. (54) is the same.

Following [18] we define the local contribution generated by vector resonance exchange a_V as

$$a_V = -\frac{\pi}{2G_8 m_K^2 \alpha_{em}} \lim_{z \rightarrow 0} B_V(z) \quad , \quad (55)$$

where $B_V(z)$ is the vector resonance contribution to the B amplitude. In [18] two sources for a_V were discussed :

$$a_V = a_V^{ext} + a_V^{dir} \quad , \quad (56)$$

that is i) strong vector resonance exchange with an external weak transition (a_V^{ext}) as in Fig. 1.a and Fig. 1.b, ii) direct vector resonance exchange between a weak and a strong $VP\gamma$ vertices (a_V^{dir}) as in Fig. 1.c and Fig. 1.d. The BMS model suggests the existence of a further a_V^{dir} contribution as given by the diagram in Fig. 1.e.

The contribution to a_V from Vector Resonance exchange between two strong vertices supplemented with a weak transition in an external leg (Figs. 1.a and 1.b) is very well determined phenomenologically due to our good understanding of the strong sector involved. This we call the *external* contribution (a_V^{ext}) and has been worked out in [18] (we write the subscript 0 for the neutral channel $K_L \rightarrow \pi^0 \gamma \gamma$: $a_{V,0}$; and the subscript + for the charged channel $K^+ \rightarrow \pi^+ \gamma \gamma$: $a_{V,+}$) :

$$a_{V,0}^{ext} = \frac{512\pi^2}{9} h_V^2 \frac{m_K^2}{m_V^2} \simeq 0.32 \quad , \quad (57)$$

$$a_{V,+}^{ext} = -\frac{128\pi^2}{9} h_V^2 \frac{m_K^2}{m_V^2} \simeq -0.08 \quad ,$$

where h_V is given in Eq. (15) and we have used $m_V = m_\rho$ for the numerical evaluation.

The second contribution (a_V^{dir}) depends on the model for the direct $VP\gamma$ vertex, but the general structure (contributing to the processes of our interest) is the one provided by \mathcal{L}_6^W Eq. (54) with the following expression :

$$a_{V,0}^{dir} = -\frac{128\pi^2}{9} h_V \frac{m_K^2}{m_V^2} [2\kappa_1 + 4\kappa_2 - 3\kappa_3 + 3\kappa_4 + 3\kappa_5] \quad , \quad (58)$$

$$a_{V,+}^{dir} = -\frac{128\pi^2}{9} h_V \frac{m_K^2}{m_V^2} [\kappa_1 - \kappa_2] \quad .$$

4.2 $K_L \rightarrow \gamma\gamma^*$

We can also use our weak effective vertex $VP\gamma$ Eqs. (51, 52) to evaluate its contribution to the slope of the form factor $f(x)$ in Eqs. (43, 44).

The slope b gets two different contributions:

$$b = b_V + b_D \quad , \quad (59)$$

i) the first one (b_V) comes from the strong vector interchange with the weak transition in the K_L leg as shown in Fig. 2.b, ii) a direct weak transition $K_L \rightarrow V\gamma$ (b_D) as in Fig. 2.c. In [10] the direct transition was constructed as in Fig. 2.d, i.e. with a weak vector–vector transition (BMS model).

The evaluation of b_V is straightforward [50]⁹. By integrating out the vector mesons between two vertices generated respectively by $\mathcal{L}(VP\gamma)$ Eq. (15) and $\mathcal{L}(V\gamma)$ Eq. (17) and assuming nonet symmetry in the pseudoscalar sector we get the effective lagrangian

$$\mathcal{L}_{VMD}^6 = \frac{16\sqrt{2}}{3} \pi \alpha_{em} \frac{h_V f_V}{F_\pi m_V^2} \varepsilon_{\nu\lambda\alpha\beta} F^{\alpha\beta} \partial_\mu F^{\mu\nu} \partial^\lambda \left(\pi^0 + \frac{\eta_8}{\sqrt{3}} + 2\sqrt{\frac{2}{3}} \eta_1 \right) \quad . \quad (60)$$

Since the slope is normalized by $A(K_L \rightarrow \gamma\gamma)$, this lagrangian has to be compared with the one generated by Eq. (10) :

$$\mathcal{L}_{WZW} = -\frac{\alpha_{em}}{8\pi F_\pi} \varepsilon_{\mu\nu\alpha\beta} F^{\mu\nu} F^{\alpha\beta} \left(\pi^0 + \frac{\eta_8}{\sqrt{3}} + 2\sqrt{\frac{2}{3}} \eta_1 \right) \quad . \quad (61)$$

⁹ Ecker's definition r_V relates with our b_V through $b_V = r_V m_K^2 / m_V^2$.

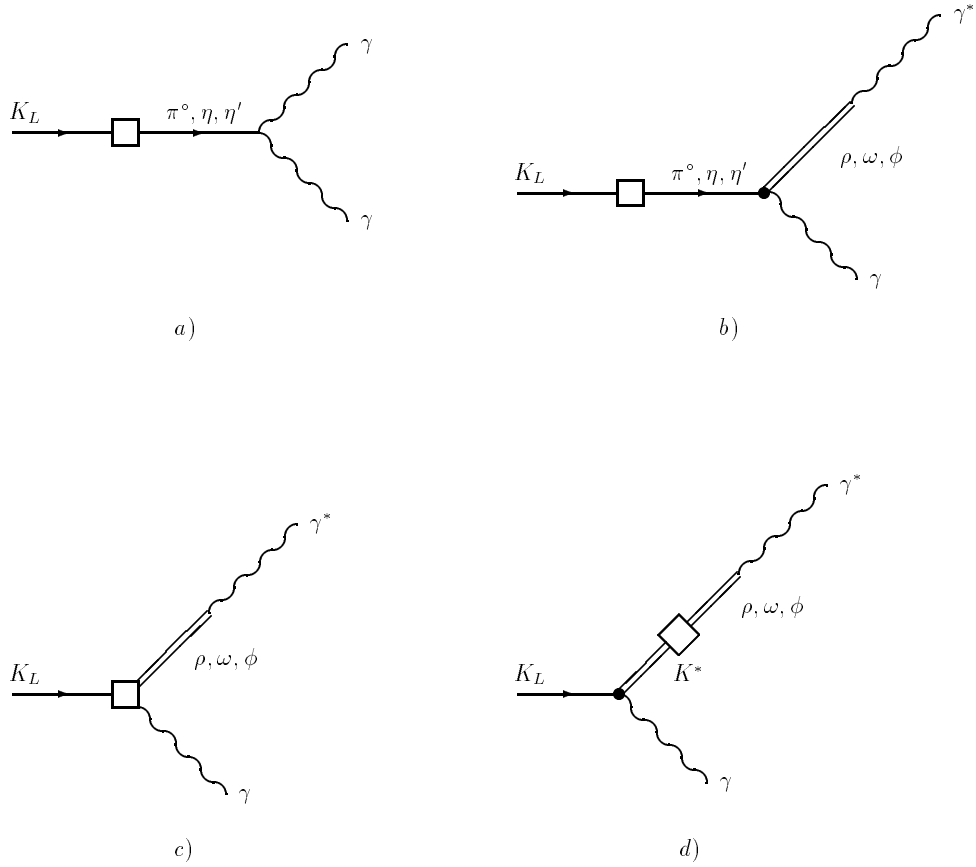


Figure 2: Feynman diagrams for $K_L \rightarrow \gamma\gamma^*$. a) corresponds to the pole model contribution to both photons on-shell, b) represents the *external* weak transitions, c) the *direct* weak transition and d) is the contribution of the BMS model to the *direct* weak transition.

Implementing the external weak transition $K_L \rightarrow \pi^0, \eta, \eta'$ as given by Eq. (27) (extended to $U(3) \otimes U(3)$) and normalizing with the amplitude $K_L \rightarrow \gamma\gamma$ (Fig. 2.a) we get for b_V a result independent from weak interaction parameters

$$b_V^{nonet} = \frac{32\sqrt{2}}{3} \pi^2 f_V h_V \frac{m_K^2}{m_V^2} \simeq 0.46 \quad , \quad (62)$$

and the condition $h_V f_V > 0$ from $\pi^0 \rightarrow \gamma\gamma^*$ gives $b_V > 0$. It has to be noted that this result for b_V is entirely due to the singlet η_1 contribution. This is so because the Gell-Mann–Okubo mass relation cancels the π^0 and η_8 contribution and then

$$b_V^{octet} = 0 \quad . \quad (63)$$

Violations of the mass relation or contribution from the η - η' mixing are at higher chiral order. For consistency we think one should assume nonet or octet realizations simultaneously in b_D and b_V .

We can parameterize b_D in the general framework using Eqs. (17, 51) as

$$b_D = -\frac{64\sqrt{2}}{9} \pi G_8 \alpha_{em} F_\pi f_V \frac{m_K^2}{m_V^2} \frac{1}{|A_{\gamma\gamma}^{exp}|} [\kappa_1 + 2\kappa_2 + 3\kappa_3] \quad . \quad (64)$$

By comparing the expression of $a_{V,0}^{dir}$ in Eq. (58) and b_D in Eq. (64) we can get a general relation between both observables $a_{V,0}^{dir}$ and b_D as

$$\frac{a_{V,0}^{dir}}{b_D} = \sqrt{2} \pi \frac{h_V}{f_V} \frac{|A_{\gamma\gamma}^{exp}|}{G_8 F_\pi \alpha_{em}} \frac{2\kappa_1 + 4\kappa_2 - 3\kappa_3 + 3\kappa_4 + 3\kappa_5}{\kappa_1 + 2\kappa_2 + 3\kappa_3} \quad . \quad (65)$$

Finally, it has to be taken into account that, at $\mathcal{O}(p^6)$, there is a chiral loop contribution to the slope. Nevertheless it should be very suppressed [51, 50].

5 Model predictions for $K \rightarrow \pi\gamma\gamma$

Cohen, Ecker and Pich have shown that unitarity corrections from $K_L \rightarrow \pi^0\pi^+\pi^-$ and vector meson exchange with $a_{V,0} \simeq -0.9$ [15] restore the agreement with experiment. Actually, as we will show later, the inclusion of the experimental $\gamma\gamma \rightarrow \pi^0\pi^0$ suggested in [49] decreases this value to about $a_{V,0} \simeq -0.8$. The comparative analysis with $K^+ \rightarrow \pi^+\gamma\gamma$, which is going to be measured soon at BNL-787, should establish the dominance of the computed $\mathcal{O}(p^6)$ contributions and, simultaneously, the value of \hat{c} in Eq. (46) and thus a_V should be determined.

As we have already emphasized the main source of uncertainty in the evaluation of $\mathcal{O}(p^6)$ local counterterms generated by vector resonance exchange resides in our poor knowledge of the direct weak $VP\gamma$ vertex. The prediction of the WDM for a_V^{dir} was given in [18]. Here we review that result and consider the application of FM and BMS

models. As we will see only the WDM can give a definite numerical prediction for a_V^{dir} . Our purpose will be to combine the phenomenology of both processes $K \rightarrow \pi\gamma\gamma$ and $K_L \rightarrow \gamma\gamma^*$ in order to get definite numerical predictions also from FM and BMS models. This we will do in Section 7.

5.1 Weak Deformation Model

The WDM gives a definite prediction for a_V^{dir} . This is (for an octet current) [18]

$$\begin{aligned} a_{V,0}^{dir} &= -2 a_{V,0}^{ext} , \\ a_{V,+}^{dir} &= -a_{V,+}^{ext} , \end{aligned} \tag{66}$$

showing a strong cancellation that is complete for $K^+ \rightarrow \pi^+\gamma\gamma$.

5.2 Factorization Model

For $K \rightarrow \pi\gamma\gamma$ the FM lagrangian density is

$$\mathcal{L}_{FM} = 4 k_F G_8 \left\langle \lambda \left\{ \frac{\delta S_2^X}{\delta \ell^\mu}, \frac{\delta S_V^{PP\gamma\gamma}}{\delta \ell_\mu} \right\} \right\rangle + h.c. , \tag{67}$$

where S_2^X is the action associated to the leading $\mathcal{O}(p^2)$ strong χ PT lagrangian Eq. (8) and $S_V^{PP\gamma\gamma}$ is the action of the strong $\mathcal{O}(p^6)$ lagrangian obtained by integrating out the vector mesons between two vertices generated by $\mathcal{L}(VP\gamma)$ in Eq. (15). In Eq. (67) the left-handed current associated to $S_V^{PP\gamma\gamma}$ is not automatically traceless. Since we are considering only octet currents in our evaluation we have subtracted the trace term¹⁰.

Then we find

$$\begin{aligned} a_{V,0}^{dir} &= -4 k_F a_{V,0}^{ext} , \\ a_{V,+}^{dir} &= -2 k_F a_{V,+}^{ext} . \end{aligned} \tag{68}$$

As $k_F > 0$, the FM (as the WDM) predicts a cancellation between both contributions to a_V . Comparing with Eq. (66) we see that both models give the same result for $k_F = 1/2$.

5.3 BMS model

The basic idea of the BMS model [10] is to suggest that the structure of the weak $VP\gamma$ vertex is dominated by a weak vector–vector transition as shown in Fig. 1.e. That is, for example, the $K\rho\gamma$ coupling would be generated through the sequence $K \rightarrow K^*\gamma$,

¹⁰We thank G. Ecker for calling our attention about this point.

$K^* \rightarrow \rho$. This model was introduced in [10] in the study of the $K_L \rightarrow \gamma\gamma^*$ form factor. It is argued that the weak vector–vector transition lacks penguin contributions because of the scalar and pseudoscalar quantum numbers of the penguin operators¹¹. Following this approach we introduce the leading effective weak vector–vector transition as

$$\mathcal{L}_W(VV) = 4\beta G_8 F_\pi^2 m_V^2 \langle \Delta V_\mu V^\mu \rangle \quad , \quad (69)$$

where β is an, in principle, unknown dimensionless coupling constant that fixes the strength of the transition. Motivated by the paper of Shifman, Vainshtein and Zakharov [33], where the penguin diagram was advocated to explain the $K \rightarrow \pi\pi$ matrix elements, another basic feature of the BMS model is to assume that the weak vector–vector transition has no $\Delta I = 1/2$ enhancement and hence β can be reliably evaluated using factorization and vacuum insertion.

Therefore we can evaluate the amplitudes for $K \rightarrow \pi\gamma\gamma$ using $\mathcal{L}(VP\gamma)$ Eq. (15) and $\mathcal{L}_W(VV)$ Eq. (69), and give the following predictions for a_V :

$$a_{V,0}^{dir} = -\beta a_{V,0}^{ext} \quad , \quad (70)$$

$$a_{V,+}^{dir} = \beta a_{V,+}^{ext} \quad .$$

6 Experimental determination of the slope and model predictions for $K_L \rightarrow \gamma\gamma^*$

The experimental determination of the slope b of $K_L \rightarrow \gamma\gamma^*$ Eq. (44) has been improved recently by the data on $K_L \rightarrow \gamma e^+ e^-$ and $K_L \rightarrow \gamma \mu^+ \mu^-$ [52, 53]. Both experiments use the BMS model in order to fit the slope from the data. That is, they determine α_{K^*} defined by

$$f(x) = \frac{1}{1 - x \frac{m_K^2}{m_\rho^2}} + \frac{\alpha_{K^*}}{1 - x \frac{m_K^2}{m_{K^*}^2}} A_{K^*}(x) \quad , \quad (71)$$

with

$$A_{K^*}(x) = C_* \left[\frac{4}{3} - \frac{1}{1 - x \frac{m_K^2}{m_\rho^2}} - \frac{1}{9(1 - x \frac{m_K^2}{m_\omega^2})} - \frac{2}{9(1 - x \frac{m_K^2}{m_\phi^2})} \right] \quad , \quad (72)$$

where, as computed in [10],

$$C_* = \frac{64}{3} \pi \alpha_{em} G_F m_V^2 f_V^3 \frac{h_V}{F_\pi |A_{\gamma\gamma}^{exp}|} \quad , \quad (73)$$

¹¹The penguin $(V - A) \times (V + A)$ structure can be Fierz ordered to $(SS - PP)$.

which numerical value is $C_* \simeq 3.1$ for $m_V = m_\rho$. However we will use the numerical result given in [52] that includes the $SU(3)$ breaking $C_* = 2.5$. From the data the value of α_{K^*} in Eq. (71) can be extracted and it is

$$\begin{aligned}\alpha_{K^*} &= -0.28 \pm 0.13 \quad , \quad [K_L \rightarrow \gamma e^+ e^-, [52]] \\ \alpha_{K^*} &= -0.03 \pm 0.11 \quad , \quad [K_L \rightarrow \gamma \mu^+ \mu^-, [53]] \quad .\end{aligned}\tag{74}$$

As can be seen the experimental situation still needs improvement. We note the good agreement of the value of α_{K^*} from $K_L \rightarrow \gamma e^+ e^-$ with the prediction of the BMS model [10] $|\alpha_{K^*}| \simeq 0.2 - 0.3$.

There is no reason a priori, according to us, that the form factor in Eq. (71) should work better than just the linear expansion in Eq. (44). Actually this last one is the one suggested by χ PT. Of course Eq. (71) could be a resummation of higher order terms but it is not guaranteed to work. Deviations from the linear expansion are particularly important for $K_L \rightarrow \gamma \mu^+ \mu^-$. Thus we suggest the experimentalists to fit $K_L \rightarrow \gamma e^+ e^-$ and $K_L \rightarrow \gamma \mu^+ \mu^-$ with both Eq. (44) and Eq. (71) and then conclude which one works for both decays. Indeed if the linear slope is universal, then α_{K^*} determined from $K_L \rightarrow \gamma \mu^+ \mu^-$ should be substantially smaller than α_{K^*} measured in $K_L \rightarrow \gamma e^+ e^-$, as suggested by the experimental results in Eq. (74). As a first approximation we determine the full slope b , defined in Eq. (44), experimentally from $K_L \rightarrow \gamma e^+ e^-$ by Taylor expanding $f(x)$ in Eq. (71) and keeping only the linear slope. This gives

$$b_{exp} = 0.81 \pm 0.18 \quad .\tag{75}$$

However one should emphasize that the coefficients of the quadratic terms in Eq. (71) could be misleading since other contributions should be relevant at this chiral order ¹².

Thus assuming b_V^{nonet} in Eq. (62) we can express the slope b_D Eq. (59) in terms of α_{K^*} ,

$$b_D^{exp} = -\frac{4}{3} C_* \frac{m_K^2}{m_V^2} \alpha_{K^*} \simeq 0.39 \pm 0.18 \quad ,\tag{76}$$

where $m_\phi = m_\omega = m_\rho = m_V$ in Eqs. (71,72) has been used, and for the numerical result we have put $m_V = m_\rho$ and $\alpha_{K^*} = -0.28 \pm 0.13$ as given by the $K_L \rightarrow \gamma e^+ e^-$ data. We use this value since we think that the value of α_{K^*} from $K_L \rightarrow \gamma e^+ e^-$ is definitely a better approach for the following reason: the value of α_{K^*} is fitted using the expression Eq. (71) that has all orders in x . A quick look to the expansion in x shows that the quadratic term is not so negligible against the slope, and this is even more important in the $K_L \rightarrow \gamma \mu^+ \mu^-$ case where the average x is bigger than in $K_L \rightarrow \gamma e^+ e^-$.

¹²We have fitted a slope from the quadratic expansion of $f(x)$ in Eq. (71) and we find a 30% bigger value than the one quoted in Eq. (75).

The models considered previously can also be used to evaluate the slope b_D , defined as in Eq. (59), of the form factor for the process $K_L \rightarrow \gamma\gamma^*$. We will show the different model predictions.

The normalization specified in Eq. (43) requires we take care about our sign conventions. We use for the $K_L \rightarrow \gamma\gamma$ amplitude the same definition that in $K_L \rightarrow \gamma\gamma^*$ Eq. (42) but now $A_{\gamma\gamma^*}(0) \equiv A_{\gamma\gamma}$. From the experimental width $K_L \rightarrow \gamma\gamma$ [25] we get $|A_{\gamma\gamma}^{exp}| \simeq 3.45 \times 10^{-9} GeV^{-1}$. It is known that $K_L \rightarrow \gamma\gamma$ is dominated by long distance contributions [54]. By evaluating the diagram in Fig. 2.a given by the pole model ([54, 55, 6] and references therein) the leading $SU(3)$ $\mathcal{O}(p^4)$ contribution vanishes due to the cancellation among π^0 and η_8 . The experimental magnitude of $A_{\gamma\gamma}$ shows that $\mathcal{O}(p^6)$ contributions are very large. One could evaluate the diagram in Fig. 2.a using nonet symmetry with a mixing angle between η_8 and η_1 , $\theta_P \simeq -20^\circ$ [25] and one would get a negative sign for $A_{\gamma\gamma}$. As we shall see all the studied models require a positive value for $A_{\gamma\gamma}$ in order to reproduce the experimental sign of b_D Eq. (76). This fact let us to think that a more thorough evaluation of the poorly known $A(K_L \rightarrow \gamma\gamma)$ is needed and other $\mathcal{O}(p^6)$ contributions have to be taken into account, like a strong breaking of nonet symmetry¹³. Therefore since the pole model for $K_L \rightarrow \gamma\gamma$ does not seem to reproduce the right sign for the slope we input the sign inferred from the experimental slope.

Next we give the different model predictions for the slope $K_L \rightarrow \gamma\gamma^*$.

6.1 Weak Deformation Model

As we have said before, WDM gives a definite numerical prediction for the slope. The procedure consists in “deforming” the octet current coupled to vector mesons in $\mathcal{L}(VP\gamma)$ Eq. (15) and to integrate out the vector meson interchanged with a vertex generated by $\mathcal{L}(V\gamma)$ Eq. (17). We get from diagram in Fig. 2.c

$$b_D^{octet} = \frac{128\sqrt{2}}{9} \pi G_8 F_\pi h_V f_V \alpha_{em} \frac{m_K^2}{m_V^2} \frac{1}{|A_{\gamma\gamma}^{exp}|} \simeq 0.35 \quad . \quad (77)$$

This result has also been obtained by Ecker [50] who added it to b_V^{nonet} in Eq. (62). However we think that b_D^{octet} should be added up to $b_V^{octet} = 0$, and therefore the experimental result Eq. (75) is not recovered. Nevertheless the value of b_D^{octet} approaches the result Eq. (76). The extension to the nonet case is ambiguous for this model [38], though the consistent choice, which enlarges the equivalence theorem between $\mathcal{O}(p^4)$ FM with $k_F = 1/2$ and WDM, to the nonet, would lead to

$$b_D^{nonet} \simeq 0.70 \quad . \quad (78)$$

b_D^{nonet} added to b_V^{nonet} in Eq. (62) could still not to be excluded. In any case this is not a firm prediction of the WDM.

¹³However there is no evidence of nonet symmetry breaking in $\eta' \rightarrow \gamma\gamma$ and $\eta' \rightarrow \gamma\gamma^*$ [51].

6.2 Factorization model

In order to evaluate the slope in the factorization model we first construct the strong lagrangian generated by vector exchange between $\mathcal{L}(VP\gamma)$ Eq. (15) and $\mathcal{L}(V\gamma)$ Eq. (17). This gives

$$\mathcal{L}(P\gamma\gamma^*) = -\frac{h_V f_V}{\sqrt{2} m_V^2} \varepsilon_{\mu\nu\rho\sigma} \langle \nabla_\alpha f_+^{\alpha\mu} \{ u^\nu, f_+^{\rho\sigma} \} \rangle, \quad (79)$$

and then the FM lagrangian density for $K_L \rightarrow \gamma\gamma^*$ is

$$\mathcal{L}_{FM} = 4 k_F G_8 \langle \lambda \left\{ \frac{\delta S_2^\chi}{\delta \ell^\mu}, \frac{\delta S_V^{P\gamma\gamma^*}}{\delta \ell_\mu} \right\} \rangle + h.c., \quad (80)$$

with S_2^χ the action associated to \mathcal{L}_2 in Eq. (8) and $S_V^{P\gamma\gamma^*}$ is the action associated to $\mathcal{L}(P\gamma\gamma^*)$ Eq. (79). As in Eq. (67) we are assuming octet currents and therefore $\langle \delta S_V^{P\gamma\gamma^*} / \delta \ell_\mu \rangle$ has to be extracted in Eq. (80). We get for the octet case

$$b_D^{octet} = \frac{256\sqrt{2}}{9} \pi G_8 F_\pi h_V f_V \alpha_{em} \frac{m_K^2}{m_V^2} \frac{1}{|A_{\gamma\gamma}^{exp}|} k_F, \quad (81)$$

while for the nonet

$$b_D^{nonet} = 2 b_D^{octet}. \quad (82)$$

We note that as $h_V f_V > 0$, $b_D > 0$ for $k_F > 0$. Moreover, for $0 < k_F < 1$ we find $0 < b_D^{octet} < 0.71$, $0 < b_D^{nonet} < 1.42$. The upper limit corresponds to nFM ($k_F = 1$). Hence adding b_D to b_V in Eq. (63) and Eq. (62), respectively, one finds that the octet case is not excluded for $k_F \simeq 1$, while the nonet is good for small values of k_F . We remark that $k_F = 1/2$ recovers the result of b_D^{octet} in the WDM.

6.3 BMS model

Using the weak vector–vector effective vertex defined in Eq. (69), $\mathcal{L}(VP\gamma)$ Eq. (15) and $\mathcal{L}(V\gamma)$ Eq. (17) we can evaluate the slope in the BMS model. It reads

$$b_D = \frac{512\sqrt{2}}{9} \pi G_8 F_\pi h_V f_V \alpha_{em} \frac{m_K^2}{m_V^2} \frac{1}{|A_{\gamma\gamma}^{exp}|} \beta. \quad (83)$$

Bergström, Massó and Singer [10] evaluated the dimensionless coupling β using factorization and vacuum insertion in order to obtain the weak vector–vector matrix element, as mentioned earlier. They got $|\beta| \simeq 0.2 - 0.3$. In fact by comparing Eq. (83) with Eq. (76) we obtain

$$\beta \simeq -\alpha_{K^*} = 0.28 \pm 0.13. \quad (84)$$

From the experimental value of α_{K^*} we see that the magnitude of the coupling β predicted in [10] is in good agreement with the experiment on the channel $K_L \rightarrow \gamma e^+ e^-$.

7 FM and BMS model predictions for $K_L \rightarrow \gamma\gamma^*$ and $K \rightarrow \pi\gamma\gamma$

As we saw in Section 5 both FM and BMS models determine the parameter a_V Eq. (55) in terms of their unknown couplings k_F and β , respectively, *a priori* unknown.

Our strategy is to determine k_F and β from $K_L \rightarrow \gamma\gamma^*$. Regarding the FM three possible routes are available according to the description of the slope parameter b . We could compare our expressions for b_D in Eqs. (81,82) with b_D^{exp} in Eq. (76). However the determination of b_D^{exp} in Eq. (76) is very much model dependent. In order to minimize this dependence we are forced to compare with $b_{exp} - b_V$ in Eqs. (75,62,63) instead. We get

$$\begin{aligned} b_{exp} - b_V^{octet} &= b_D^{octet} \longrightarrow k_F = 1.15 \pm 0.25 \quad , \\ b_{exp} - b_V^{nonet} &= b_D^{nonet} \longrightarrow k_F = 0.25 \pm 0.13 \quad , \\ b_{exp} - b_V^{nonet} &= b_D^{octet} \longrightarrow k_F = 0.49 \pm 0.25 \quad . \end{aligned} \tag{85}$$

(We stress that the last relation corresponds to a *mixed* octet–nonet scheme). For the BMS model we have, from Eq. (84),

$$\beta = -\alpha_{K^*} \simeq 0.28 \quad . \tag{86}$$

Then $a_{V,0}^{dir}$ is computed from Eqs. (68,70) in the FM and BMS models. These results and the WDM predictions are collected in Table 1.

Indeed the pure *FM* nonet solution in Eq. (85) gives a very small value of k_F unacceptable for $K_L \rightarrow \pi^0\gamma\gamma$. The first solution (pure octet) seems more reasonable from a theoretical point of view and even more so since it gives an acceptable value for $a_{V,0}$.

As we can see from the results in the Table 1, the prediction for a_V of the WDM and FM are consistent for $K^+ \rightarrow \pi^+\gamma\gamma$ showing a strong cancellation. The situation for $K_L \rightarrow \pi^0\gamma\gamma$ is more articulated. Both WDM and FM also predict a cancellation between *direct* and *external* contributions. This cancellation is bigger in the *mixed* scheme of the FM (but we note the $\sim 50\%$ error in the determination of k_F Eq. (85) that affects linearly to a_V^{dir} from FM). As it can be seen the BMS model contribution is very small in both channels. Only the FM model in the *octet* scheme predicts a large value for $a_{V,0}$ that seems to be demanded from the phenomenology [15] as we shall see in Section 9.1. Alternatively we could use the value $a_{V,0} \simeq -0.9$ in order to get the parameters k_F and β and then through the use of Eq. (85) give a prediction for α_{K^*} . However from the poor result of the predictions of $a_{V,0}^{dir}$ from the BMS model in Table 1 we realize that the predicted value for α_{K^*} is going to be larger than the experimental result in Eq. (74). In fact we find $k_F \simeq 0.95$ and $\beta \simeq 3.81$ to compare with Eq. (85) and Eq. (86) respectively. We conclude then that the BMS model is not able to give a consistent picture of both

Channel	a_V^{ext}	a_V^{dir}				$a_V = a_V^{ext} + a_V^{dir}$		
		WDM	FM	BMS	FMV	WDM	FM	FMV + BMS
$K_L \rightarrow \pi^0 \gamma \gamma$	0.32	-0.64	$-1.28 k_F$	-0.09	-0.95	-0.32	$0.32 - 1.28 k_F$	-0.72
$K^+ \rightarrow \pi^+ \gamma \gamma$	-0.08	0.08	$0.16 k_F$	-0.02	-0.05	0	$0.16 k_F - 0.08$	-0.15

Table 1: Results for a_V^{dir} from WDM, FM, BMS and FMV models and final result for the a_V parameter in both $K_L \rightarrow \pi^0 \gamma \gamma$ and $K^+ \rightarrow \pi^+ \gamma \gamma$ channels. The result of the FMV model is for $\eta = 0.21$ as given in Eq. (92). For the FM results the values of k_F would be the ones in Eq. (85) for the different schemes : nonet, octet or *mixed*.

processes while the FM gives from the phenomenological $a_{V,0}$ a slope $b_D^{octet} \simeq 0.66$ that still can be consistent with the expected value.

It should be noticed that one could be tempted to add both FM and BMS contributions since they seem generated by different dynamical mechanisms. However, in the next Section we will show that indeed there are even other contributions to be taken into account, so we have preferred to analyse the predictions of the FM model as originally introduced in [20].

8 Factorizable Wess–Zumino–Witten anomaly contribution from vector resonances to $K \rightarrow \pi\gamma\gamma$ and $K_L \rightarrow \gamma\gamma^*$

The procedure used in the FM to study the resonance exchange contribution to a specified process involves first the construction of a resonance exchange generated strong Lagrangian, in terms of Goldstone bosons and external fields, from which to evaluate the left-handed currents. For example, in $K \rightarrow \pi\gamma\gamma$ one starts from the strong $VP\gamma$ vertex and integrates out the vector mesons between two of those vertices giving a strong Lagrangian for $PP\gamma\gamma$ (P is short for pseudoscalar meson) from which to evaluate the left-handed current. This method of implementing the FM imposes as a constraint the strong effective $PP\gamma\gamma$ vertex and therefore it can overlook parts of the chiral structure of the weak vertex. In the FM model the dynamics is hidden in the fudge factor k_F . Alternatively one could try to identify the different vector meson exchange contributions and then estimate the relative weak couplings.

We propose to work out the factorizable contributions for the processes of our interest. Instead of getting the strong lagrangian generated by vector meson exchange we apply the factorization procedure to the construction of the weak $VP\gamma$ vertex and we integrate out the vector mesons afterwards. The interesting advantage of our approach is that, as we will see in the processes we are interested in, allows us to identify new contributions to the left-handed currents and therefore to the chiral structure of the weak amplitudes.

Let us specify the procedure. For later use we will split the strong effective action S and the corresponding left-handed current \mathcal{J}_μ in two pieces : $S = S_1 + S_2$ and $\mathcal{J}_\mu = \mathcal{J}_\mu^1 + \mathcal{J}_\mu^2$, respectively. The bosonization of the four-quark operators in $\mathcal{H}_{NL}^{\Delta S=1}$ proposed in [20] and specified in Eq. (32) tells us

$$\overline{q_l}\gamma^\mu(1-\gamma_5)q_k\overline{q_j}\gamma_\mu(1-\gamma_5)q_i \longleftrightarrow 4[(\mathcal{J}_\mu^1)_{lk}(\mathcal{J}_2^\mu)_{ji} + (\mathcal{J}_\mu^2)_{lk}(\mathcal{J}_1^\mu)_{ji}] \quad , \quad (87)$$

with i, j, k, l flavour indices (terms $\mathcal{J}_\mu^1\mathcal{J}_1^\mu$ or $\mathcal{J}_\mu^2\mathcal{J}_2^\mu$ have been dropped since they will not contribute to the processes we are considering as we shall see later). It can be shown that,

in this factorizable approach, the Q_- operator defined in Eq. (22) is represented by

$$Q_- \longleftrightarrow 4 \left[\langle \lambda \{ \mathcal{J}_\mu^1, \mathcal{J}_2^\mu \} \rangle - \langle \lambda \mathcal{J}_\mu^1 \rangle \langle \mathcal{J}_2^\mu \rangle - \langle \lambda \mathcal{J}_\mu^2 \rangle \langle \mathcal{J}_1^\mu \rangle \right] , \quad (88)$$

where, for generality, the currents have been supposed to have non-zero trace¹⁴.

If we want to apply this procedure in order to construct the factorizable contribution to the $\mathcal{O}(p^3)$ weak $VP\gamma$ vertex we have to identify in the full strong action which pieces (at this chiral order) can contribute. Moreover for $K \rightarrow \pi\gamma\gamma$ and $K_L \rightarrow \gamma\gamma^*$ we are interested in a weak $VP\gamma$ vertex with the Levi-Civita antisymmetric pseudotensor.

According to our study it turns out that there are four terms in the strong action to take into account and which Lagrangian density is given in Eqs. (8,10,15 and 17). Analogously to the specified procedure we define correspondingly

$$\begin{aligned} S &= S_V + S_\varepsilon , \\ S_V &= S(V\gamma) + S_2^x , \\ S_\varepsilon &= S_{WZW} + S(VP\gamma) , \end{aligned} \quad (89)$$

where the notation is self-explicative. Constructing the left-handed currents and keeping only the terms of interest we get

$$\begin{aligned} \frac{\delta S_V}{\delta \ell_\mu} &= -\frac{f_V}{\sqrt{2}} m_V^2 u^\dagger V^\mu u - \frac{1}{2} F_\pi^2 u^\dagger u^\mu u , \\ \frac{\delta S_\varepsilon}{\delta \ell_\mu} &= \varepsilon^{\mu\nu\alpha\beta} \left[\frac{1}{16\pi^2} \left\{ F_{\nu\alpha}^L + \frac{1}{2} U^\dagger F_{\nu\alpha}^R U , u^\dagger u_\beta u \right\} + h_V u^\dagger \{ f_{\nu\alpha}^+ , V_\beta \} u \right] . \end{aligned} \quad (90)$$

Note that if we are assuming nonet symmetry in the vector meson sector the first term in $\delta S_V/\delta \ell_\mu$ is not traceless. The first term in $\delta S_\varepsilon/\delta \ell_\mu$ obtained from the Wess-Zumino-Witten action Eq. (10) is not traceless either, (because the anomalous breaking of the chiral symmetry), while the last term in $\delta S_\varepsilon/\delta \ell_\mu$ has to be taken traceless or not according to the inclusion of octet or nonet currents respectively. We will discuss these cases later on. From Eq. (90) we see that when the first term of the first current couples with the first term of the second current and the second terms correspondingly, we get two different contributions to the weak $VP\gamma$ vertex.

By applying the factorization procedure Eq. (88) to our currents Eq. (90) we get our effective action

$$\begin{aligned} \mathcal{L}_W^{fact}(VP\gamma) &= 4 G_8^{eff} \left[\langle \lambda \left\{ \frac{\delta S_V}{\delta \ell^\mu} , \frac{\delta S_\varepsilon}{\delta \ell_\mu} \right\} \rangle - \langle \lambda \frac{\delta S_V}{\delta \ell^\mu} \rangle \langle \frac{\delta S_\varepsilon}{\delta \ell_\mu} \rangle \right. \\ &\quad \left. - \langle \lambda \frac{\delta S_\varepsilon}{\delta \ell^\mu} \rangle \langle \frac{\delta S_V}{\delta \ell_\mu} \rangle \right] + h.c. . \end{aligned} \quad (91)$$

¹⁴A similar procedure in the study of the chiral anomaly in non-leptonic weak interactions was used in [56].

In Eq. (91) we have defined the effective coupling G_8^{eff} , since it does not necessarily coincide with G_8 in Eq. (29). This is a free coupling in our model. For definiteness and, as we shall see, consistently with phenomenology, we use for G_8^{eff} the naive value that would arise from the $C_-(m_\rho)$ Wilson coefficient (with $\mathcal{O}(\alpha_s)$ corrections included) in Eq. (30), i.e.

$$G_8^{eff} = \eta G_8 \quad , \quad (92)$$

$$\eta = \frac{g_8^{sd}}{|g_8|} \simeq 0.21 \quad ,$$

with g_8^{sd} and g_8 defined in Eqs. (30,29) respectively. That is we do not input any $\Delta I = 1/2$ enhancement in our model. However there is no reason *a priori* for this choice (but neither to exclude) and one could keep this as a free parameter analogously to k_F in the FM model. We call our model prescribed by Eqs. (91, 92) the Factorization Model in the Vector couplings (FMV).

By inputting Eq. (90) into Eq. (91), expanding and comparing with $\mathcal{L}_W(VP\gamma)$ in Eq. (51) we can determine the contributions of our FMV model to the couplings $\kappa_i, i = 1, 2, 3, 4, 5$ defined in Eq. (52). In order to simplify our expressions we define

$$\ell_V \equiv \frac{3}{16\sqrt{2}\pi^2} f_V \frac{m_V^2}{F_\pi^2} \quad . \quad (93)$$

Then, assuming only octet currents (i.e. the term in h_V in the second current of Eq. (90) is made traceless) we get

$$\begin{aligned} \kappa_1^{FMV} &= 0 \quad , \\ \kappa_2^{FMV} &= (2h_V - \ell_V) \eta \quad , \\ \kappa_3^{FMV} &= -\frac{8}{3} h_V \eta \quad , \\ \kappa_4^{FMV} &= 2\ell_V \eta \quad , \\ \kappa_5^{FMV} &= 2\ell_V \eta \quad , \end{aligned} \quad (94)$$

while if we assume nonet currents only κ_3 changes and it becomes

$$\kappa_3^{FMV}|_{nonet} = -4h_V \eta \quad . \quad (95)$$

With these results we can give now a prediction from the FMV model to both a_V^{dir} Eq. (58) in $K \rightarrow \pi\gamma\gamma$ and the slope b_D in Eq. (64).

For $K \rightarrow \pi\gamma\gamma$ we input in the Eq. (58) the values of κ_i^{FMV} corresponding to the octet currents Eq. (94). We get

$$a_{V,0}^{dir}|_{FMV} = -\frac{1024\pi^2}{9} h_V \frac{m_K^2}{m_V^2} [2h_V + \ell_V] \eta \simeq -0.95 \quad , \quad (96)$$

$$a_{V,+}^{dir}|_{FMV} = -\frac{128\pi^2}{9} h_V \frac{m_K^2}{m_V^2} [\ell_V - 2h_V] \eta \simeq -0.05 \quad .$$

In the same way using Eq. (64) we can give a prediction for the slope b_D of $K_L \rightarrow \gamma\gamma^*$. Here for the purpose of our later discussion we consider both octet Eq. (94) or the κ_3^{FMV} from Eq. (95) in the nonet current case. We get :

$$b_D^{octet} |_{FMV} = \frac{128\sqrt{2}}{9} \pi G_8 \alpha_{em} F_\pi f_V \frac{m_K^2}{m_V^2} \frac{1}{|A_{\gamma\gamma}^{exp}|} [2h_V + \ell_V] \eta \simeq 0.51 ,$$

$$b_D^{nonet} |_{FMV} = \frac{128\sqrt{2}}{9} \pi G_8 \alpha_{em} F_\pi f_V \frac{m_K^2}{m_V^2} \frac{1}{|A_{\gamma\gamma}^{exp}|} [4h_V + \ell_V] \eta \simeq 0.66 .$$
(97)

Before proceeding on, it is worth to remark the similarities and differences between our FMV and the usual FM approach. We have already stated above that the basic difference in our model is that we apply the FM to construct a weak $VP\gamma$ vertex and then we integrate out the vector mesons afterwards. If we take a look to $a_V^{dir}(FMV)$ in Eq. (96) and compare it with the WDM result Eq. (66) or the FM result Eq. (68) we see that the part from $a_V^{dir}(FMV)$ in h_V^2 coincides with the FM and the WDM for $\eta = 1/2$, that is $G_8^{eff} = G_8/2$ or $k_F = 1/2$ in the FM. Therefore the term in ℓ_V in $a_V^{dir}(FMV)$ Eq. (96) is a complete **new** contribution. Exactly the same applies to $b_D^{octet}(FMV)$.

The relevance of our new contribution goes in fact further than a numerical result. Let us consider the effective lagrangian for $K \rightarrow \pi\gamma\gamma$ generated by vector resonance exchange between a vertex from $\mathcal{L}_W^{fact}(VP\gamma)$ Eq. (91) and a vertex from $\mathcal{L}(VP\gamma)$ in Eq. (15). We arrive to

$$\begin{aligned} \mathcal{L}_{eff}^{K \rightarrow \pi\gamma\gamma} = & 4\pi\alpha_{em} h_V G_8^{eff} \frac{F_\pi^2}{m_V^2} \left[\varepsilon^{\mu\nu\alpha\beta} \varepsilon_{\mu\gamma\delta\epsilon} \right] \cdot \\ & \left[(\ell_V - 2h_V) \langle \{u_\nu, f_{\alpha\beta}^+\} \{ \{\Delta, u^\gamma\}, f_+^{\delta\epsilon} \} \rangle \right. \\ & + \frac{8}{3} h_V \langle \Delta u^\gamma \rangle \langle f_+^{\delta\epsilon} \{ u_\nu, f_{\alpha\beta}^+ \} \rangle \\ & \left. - 4\ell_V \langle \Delta \{ u_\nu, f_{\alpha\beta}^+ \} \rangle \langle f_+^{\delta\epsilon} u^\gamma \rangle \right] . \end{aligned}$$
(98)

As can be seen the last term in Eq. (98) is only proportional to ℓ_V and therefore it gives a new chiral structure operator to the process that has not been taken into account before. This is particularly evident from formulae in Eq. (96) for $a_{V,0}$ and $a_{V,+}$ where different Clebsch–Gordan relations weight the terms proportional to ℓ_V and h_V . This model proves to be more efficient than the usual FM approach in that it is able to identify a new chiral structure that contributes to both $K \rightarrow \pi\gamma\gamma$ and $K_L \rightarrow \gamma\gamma^*$. When this piece is included we find that a consistent picture of these channels arises. In particular, we find agreement between the phenomenologically expected $\mathcal{O}(p^6)$ vector meson contribution to $K_L \rightarrow \pi^0\gamma\gamma$ and our prediction.

It is interesting to note that our FMV model result in Eq. (90) can also be derived in the Hidden symmetry formulation of vector mesons [27] (see the Appendix). As already noticed previously [51] the phenomenological value of h_V can be nicely reproduced by

the so called “complete vector meson dominance”. As we show in the Appendix, in this scheme one obtains also the following relation

$$\ell_V = 4 h_V \quad , \quad (99)$$

phenomenologically consistent. Then our results can be easily derived. Thus, from this point of view, the Hidden symmetry formulation with “complete vector meson dominance” seems a complete and predictive framework.

9 Results

In this Section we are going to collect and discuss our results. In our approach we add the different vector meson exchange contributions to the processes under consideration. We have already seen that the BMS model by itself only can account for the slope b_D in $K_L \rightarrow \gamma\gamma^*$ but not for $a_{V,0}$ in $K_L \rightarrow \pi^0\gamma\gamma$. In fact if we compare diagrams in Fig. 1.c (with a direct weak $VP\gamma$ vertex) and in Fig. 1.e (with the weak V–V transition, BMS model) (or Fig. 2.c with Fig. 2.d) we realize that both contributions are independent because they have different physical mechanism and analytical structure (the BMS amplitude has an extra pole due to the two vector propagators). This is the reason why we conclude that both contributions, the BMS and FMV, are independent and therefore should be added up. This addition is numerically relevant for $K_L \rightarrow \gamma\gamma^*$ but not in $K \rightarrow \pi\gamma\gamma$.

9.1 $K \rightarrow \pi\gamma\gamma$

Our results for a_V have been written in Table 1. As a final result we have

$$a_{V,0} = a_{V,0}^{ext} + a_{V,0}^{dir}|_{FMV} + a_{V,0}^{dir}|_{BMS} \simeq -0.72 \quad , \quad (100)$$

$$a_{V,+} = a_{V,+}^{ext} + a_{V,+}^{dir}|_{FMV} + a_{V,+}^{dir}|_{BMS} \simeq -0.15 \quad .$$

Before analyzing these results is worth repeating the analysis of Cohen, Ecker and Pich [15] but adding the contribution pointed out by Holstein and Kambor [49] due to the inclusion of the experimental value of $\gamma\gamma \rightarrow \pi^0\pi^0$. As shown in [15], once unitarity corrections are included [14, 15], a value of $a_{V,0} \simeq -0.9$ is able to reproduce well the width and spectrum of $K_L \rightarrow \pi^0\gamma\gamma$. When the experimental $\gamma\gamma \rightarrow \pi^0\pi^0$ is taken into account increasing the A amplitude by a 10% the aforementioned agreement arises for a slightly smaller value $a_{V,0} \simeq -0.8$.

For the central value of our result Eq. (100), $a_{V,0} \simeq -0.7$ we find

$$Br(K_L \rightarrow \pi^0\gamma\gamma) = 1.50 \times 10^{-6} \quad , \quad (101)$$

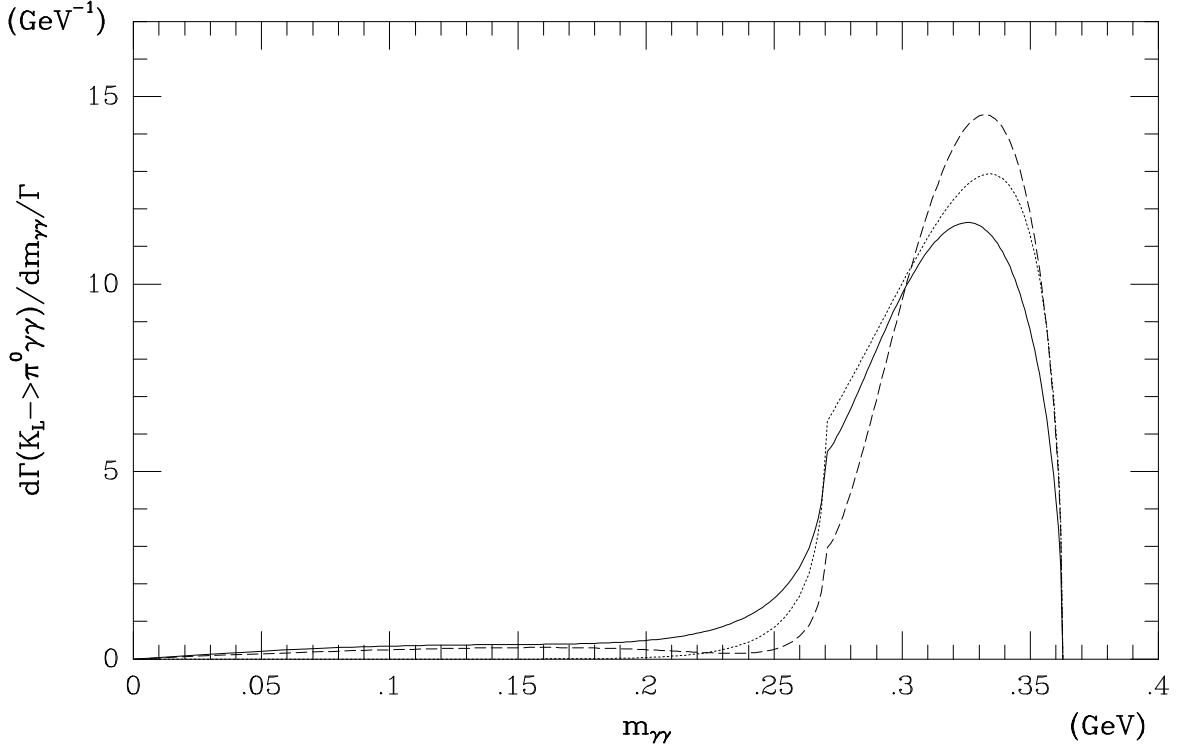


Figure 3: Normalized diphoton invariant mass spectrum for $K_L \rightarrow \pi^0 \gamma \gamma$ at $\mathcal{O}(p^4)$ (dotted line), $\mathcal{O}(p^6)$ with $a_{V,0} = 0$ (dashed line) and $\mathcal{O}(p^6)$ with $a_{V,0} = -0.7$ (full line). The $\mathcal{O}(p^6)$ curves also include the unitarity corrections from $K_L \rightarrow \pi^0 \pi^+ \pi^-$ from [14, 15] and the inclusion of experimental $\gamma \gamma \rightarrow \pi^0 \pi^0$ [49].

to be compared with the experimental world average $Br(K_L \rightarrow \pi^0 \gamma \gamma)_{exp} = (1.70 \pm 0.28) \times 10^{-6}$ [25] (see also Eq. (47)). In Fig. 3 we compare the normalized diphoton invariant mass spectrum of $K_L \rightarrow \pi^0 \gamma \gamma$ at $\mathcal{O}(p^4)$ and $\mathcal{O}(p^6)$ with $a_{V,0} = 0, -0.7$.

As already emphasized earlier, this prediction is based on taking for the parameter η Eq. (92) the central value of the Wilson coefficient in Eq. (24). Though it is a very interesting and predictive feature of the model and supported by experiment, it is not guaranteed to work. However one could fix the η parameter by the experimental slope of $K_L \rightarrow \gamma \gamma^*$ and then one would find still the same or, may be, a slightly larger value. For a complete understanding of the underlying quark dynamics one should enlarge our model to other channels and then find the effective coupling analogous to the one in Eq. (92).

In Fig. 4 we plot the diphoton invariant mass distribution of $K_L \rightarrow \pi^0 \gamma \gamma$ for three different values $a_{V,0} = -0.4, -0.7, -1.0$. This error interval is motivated either by the error in the slope of $K_L \rightarrow \gamma \gamma^*$ or our uncertainty in $C_-(m_\rho)$. Then correspondingly to

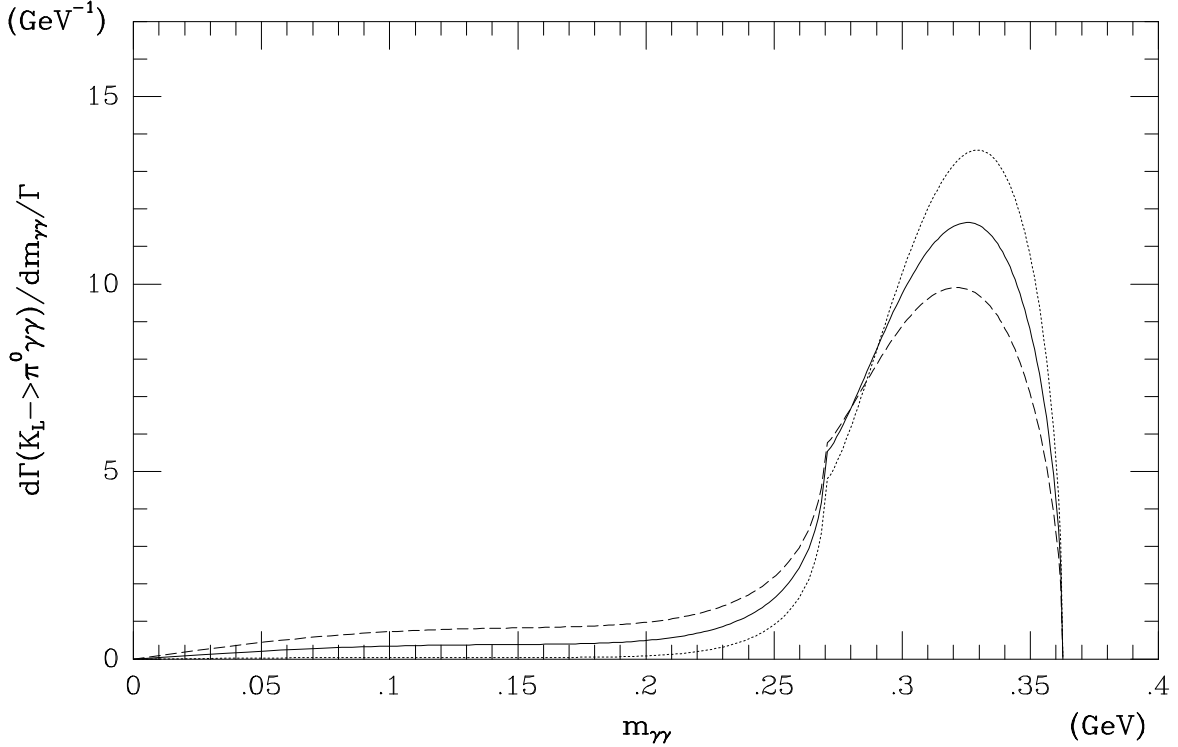


Figure 4: Normalized diphoton invariant mass spectrum for $K_L \rightarrow \pi^0 \gamma \gamma$ at $\mathcal{O}(p^6)$ (with the inclusion of the same contributions as in Fig. 3) with $a_{V,0} = -0.7$ (full line), $a_{V,0} = -0.4$ (dotted line) and $a_{V,0} = -1.0$ (dashed line).

the values of $a_{V,0}$,

$$Br(K_L \rightarrow \pi^0 \gamma \gamma) = \begin{cases} 1.12 \times 10^{-6} & , a_{V,0} = -0.4 \\ 1.50 \times 10^{-6} & , a_{V,0} = -0.7 \\ 2.06 \times 10^{-6} & , a_{V,0} = -1.0 \end{cases} , \quad (102)$$

which central value is in nice agreement with experiment. In Figs. 3 and 4 the small $m_{\gamma\gamma}$ region is interesting due to the dominance of the B amplitude. Comparing the curves for $\mathcal{O}(p^6)$ $a_{V,0} = 0$ in Fig. 3 (dashed line) with the one for $\mathcal{O}(p^6)$ $a_{V,0} = -0.4$ in Fig. 4 (dotted line) we see that there is a cancellation, for $a_{V,0} = -0.4$, between the vector resonance exchange and unitarity contributions to the B amplitude.

The discontinuity contribution of $K_L \rightarrow \pi^0 \gamma \gamma$ to the CP-conserving amplitude of $K_L \rightarrow \pi^0 e^+ e^-$ in the range of $a_{V,0}$ values considered above is

$$Br(K_L \rightarrow \pi^0 e^+ e^-) |_{abs} = \begin{cases} 0.11 \times 10^{-12} & , a_{V,0} = -0.4 \\ 1.24 \times 10^{-12} & , a_{V,0} = -0.7 \\ 3.59 \times 10^{-12} & , a_{V,0} = -1.0 \end{cases} . \quad (103)$$

This result is consistent with the values obtained in [14, 43, 48].

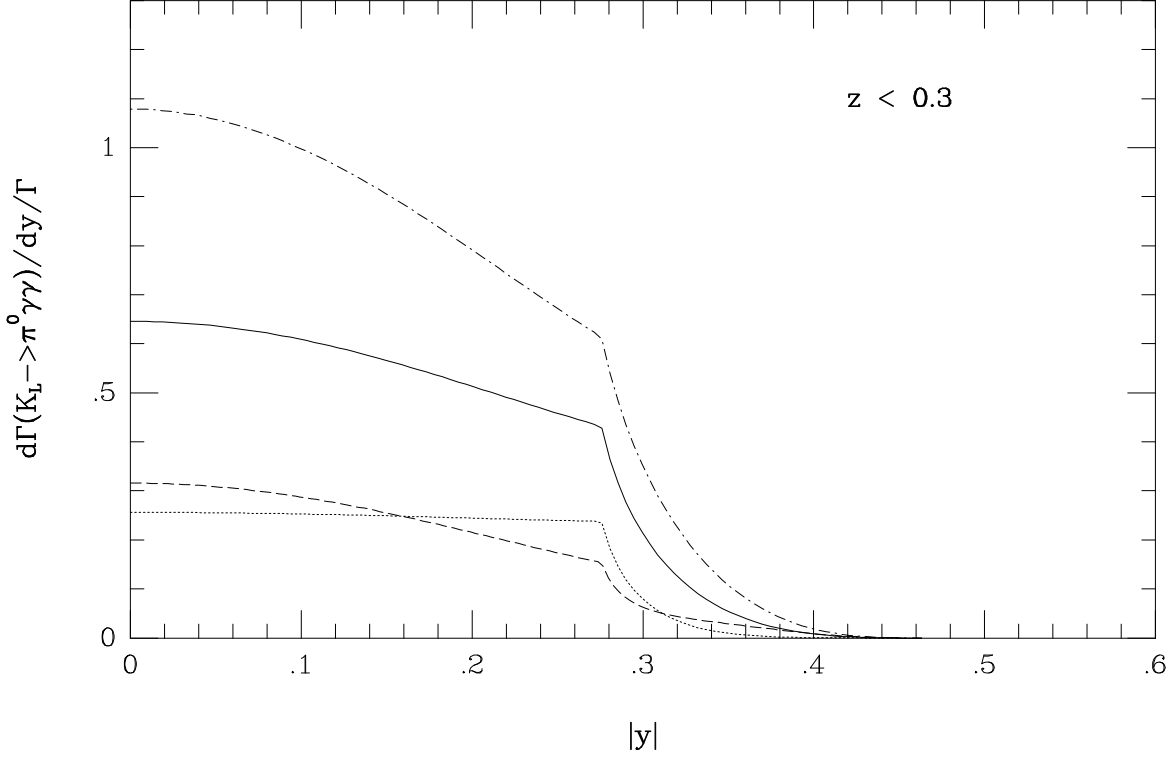


Figure 5: Normalized y -spectrum for $K_L \rightarrow \pi^0 \gamma \gamma$ and $z < 0.3$ for $a_{V,0} = 0$ (dashed line), $a_{V,0} = -0.4$ (dotted line), $a_{V,0} = -0.7$ (full line) and $a_{V,0} = -1.0$ (dash-dotted line). No cut in z is considered in the normalizing width. The corresponding branching ratios are given in Eqs. (49,102).

In $K^+ \rightarrow \pi^+ \gamma \gamma$ the situation is rather different. First there is an unknown counterterm parameter \hat{c} Eq. (46) at $\mathcal{O}(p^4)$, and then all the models coincide in giving a small value for $a_{V,+}$ that is not going to change the prediction we have already pointed out in [17] where the unitarity correction of $K^+ \rightarrow \pi^+ \pi^+ \pi^-$ has been included.

There is also another observable in $K \rightarrow \pi \gamma \gamma$ sensitive to the value of a_V . This is the y -spectrum once the variable z Eq. (38) has been cut in the upper limit. In Fig. 5 we show the normalized y -spectrum for $K_L \rightarrow \pi^0 \gamma \gamma$ and $z < 0.3$ for $a_{V,0} = 0, -0.4, -0.7, -1.0$. The dependence in a_V is manifest. The interplay between $\mathcal{O}(p^6)$ unitarity and vector meson exchange contributions that, as mentioned above, may give destructive interference, is reproduced also in Fig. 5. Indeed we notice that the behaviour of the curve for $a_{V,0} = -0.4$ is essentially equal, though different in scale, to the one that arises at $\mathcal{O}(p^4)$ [18]. In Fig. 6 we show the normalized y -spectrum for $K^+ \rightarrow \pi^+ \gamma \gamma$ with $z < 0.3$ for $\hat{c} = 0$ and $a_{V,+} = 0, -0.2$.

Ko has presented a rather involved model [21] in order to evaluate several vector meson dominated radiative kaon decays. It uses : i) a realization of vectors in the Hidden symmetry formulation; ii) assumes $\Delta I = 1/2$ enhancement, i.e. uses G_8 in Eq. (29), for

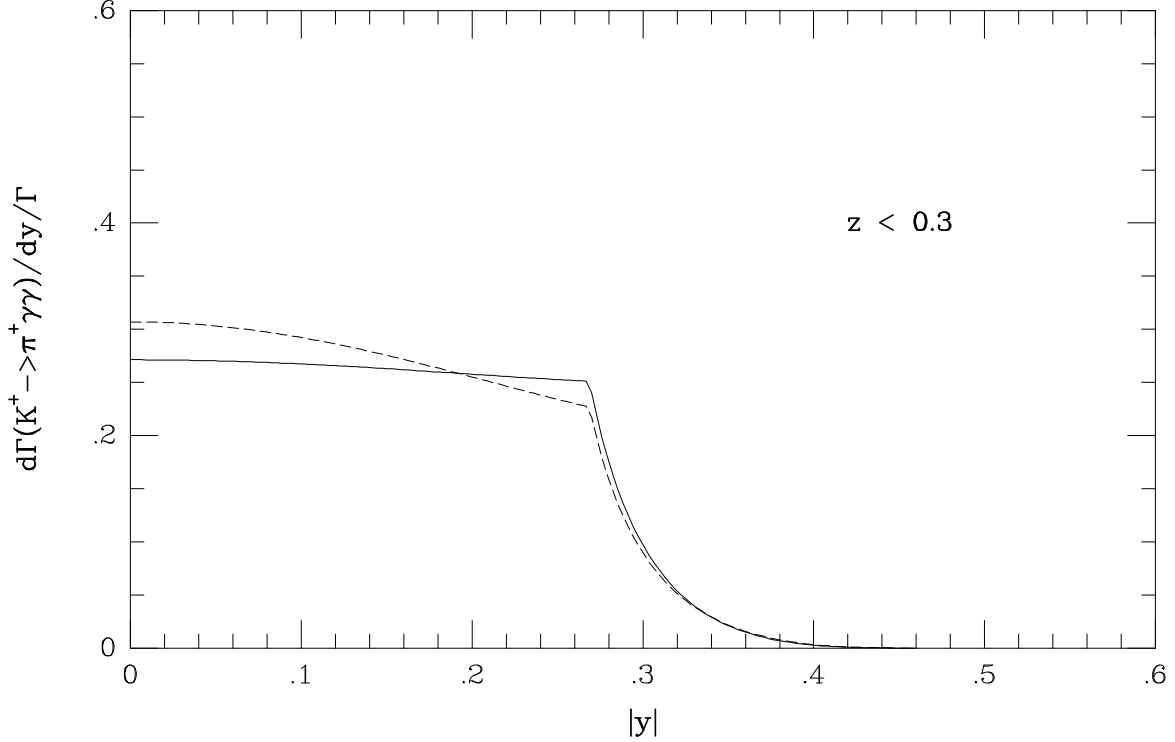


Figure 6: Normalized y -spectrum for $K^+ \rightarrow \pi^+ \gamma \gamma$ with $\hat{c} = 0$ and $z < 0.3$ for $a_{V,0} = 0$ (dashed line) and $a_{V,0} = -0.20$ (full line). The normalizing branching ratios (with no cut applied to z) are 7.24×10^{-7} and 7.52×10^{-7} respectively.

the full lagrangian (including vectors); iii) includes a free coupling in front of the second (and/or third) term in Eq. (91) that, according to the author, measures the penguin contribution; iv) the numerically very important unitarity corrections for $K \rightarrow \pi \gamma \gamma$ are not taken into account; v) uses nonet symmetry in $K_L \rightarrow \gamma \gamma^*$ and $K \rightarrow \pi \gamma \gamma$. Ko concludes that the penguin contribution is noticeable, result that is at odds with our conclusions and the idea of the BMS model : we have shown that absence of penguin contributions is compatible with no $\Delta I = 1/2$ enhancement in the processes considered. Any or several of the aforementioned points could be at the origin of our different results. Also only the octet scheme describes correctly according to us, at this order, the phenomenology while the nonet does not.

9.2 $K_L \rightarrow \gamma \gamma^*$

We have given two results for b_D in our FMV model Eq. (97) according to the consideration of including the η' (nonet currents) or not (octet currents). Even when the numerical result does not change too much for b_D the final result for the slope indeed is very different. We have collected in Table 2 the results that we subsequently explain.

If we consider the octet case, $b_V^{octet} = 0$ because the result in Eq. (62) is only due

Currents	b_V	b_D				$b = b_V + b_D$			b_{exp} [52]
		WDM	FM	BMS	FMV	WDM	FM	BMS + FMV	
octet (no η')	0	0.35	$0.71 k_F$	0.3-0.4	0.51	0.35	$0.71 k_F$	0.8-0.9	0.81 ± 0.18
nonet (η')	0.46	--	$1.41 k_F$	0.3-0.4	0.66	--	$0.46 + 1.41 k_F$	1.4-1.5	

Table 2: Results for the slope b of $K_L \rightarrow \gamma\gamma^*$ in the WDM, FM, BMS and FMV models. The result of the FMV model is for $\eta = 0.21$ as given in Eq. (92). For the slope predicted by WDM in the nonet case see the discussion in Section 6.1.

to the singlet exchange (as a consequence of the Gell-Mann–Okubo mass relation as in $K_L \rightarrow \gamma\gamma$), and adding the result of BMS and FMV models we get

$$b_{theo}^{octet} \simeq 0.8 - 0.9 \quad , \quad (104)$$

to be compared with the experimental result Eq. (75) $b_{exp} = 0.81 \pm 0.18$, while if we consider the inclusion of nonet currents b_V is given by Eq. (62) and the final result is

$$b_{theo}^{nonet} \simeq 1.4 - 1.5 \quad , \quad (105)$$

that looks definitely too large. However the inclusion of the η' amounts to the inclusion of a higher chiral order and therefore this situation would mean that a complete calculation at the new order should give cancellations for b_D .

The correlation between the slope b_D in $K_L \rightarrow \gamma\gamma^*$ and the $a_{V,0}^{dir}$ parameter in $K_L \rightarrow \pi^0\gamma\gamma$ can be nicely quantified in the FM (by eliminating k_F between Eq. (81) and Eq. (68)) or in the FMV model (by carrying our results for κ_i couplings in Eq. (94) into Eq. (65)). The result happens to be the same in both cases and we get

$$a_{V,0}^{dir} = -4\sqrt{2}\pi \frac{h_V}{f_V} \frac{|A_{\gamma\gamma}^{exp}|}{G_8 F_\pi \alpha_{em}} b_D^{octet} \quad . \quad (106)$$

We stress that $a_{V,0}^{dir}$ and b_D^{octet} in this equation only account for the FM or FMV model contributions. In our approach the BMS model contribution should be added up to the FMV model.

It is also necessary to comment that, at $\mathcal{O}(p^6)$, there is a loop contribution for $P \rightarrow \gamma\gamma^*$ that we are not including. However this correction is known to be small [51] and therefore is not due to change our final result for b more than a 10%.

Bringing back the discussion about our coupling G_8^{eff} that we consider the main source of model dependence, we have to stress that a value of G_8^{eff} much different than the one prescribed by the Wilson coefficient at $\mu = m_\rho$ Eq. (92) would spoil the slope of $K_L \rightarrow \gamma\gamma^*$ and therefore, *a posteriori*, this observable puts a constraint over G_8^{eff} .

In any case we have already commented above that the experimental result for the b slope Eq. (75) is obtained through a fit to the BMS model and doing an expansion in the x variable. We consider that this procedure might underestimate the slope.

10 Conclusions

The $\mathcal{O}(p^6)$ vector exchange contributions to the channels $K_L \rightarrow \pi^0\gamma\gamma$, $K^+ \rightarrow \pi^+\gamma\gamma$ and $K_L \rightarrow \gamma\ell^+\ell^-$ are tightly correlated due to the structure of the weak $VP\gamma$ vertex.

In $K \rightarrow \pi\gamma\gamma$ while $K^+ \rightarrow \pi^+\gamma\gamma$ is still poorly known from the experimental point of view (a situation due to change soon with the first events already collected by BNL-787 and the foreseen experiment KLOE at DAΦNE), the situation of $K_L \rightarrow \pi^0\gamma\gamma$ is much

better. As concluded in [15] it seems that $K_L \rightarrow \pi^0 \gamma \gamma$ needs a noticeable local contribution from vector exchange in order to bring agreement between theory and experiment.

The slope of $K_L \rightarrow \gamma \gamma^*$ determined experimentally from $K_L \rightarrow \gamma e^+ e^-$ can be computed using octet or nonet symmetry (η' on the same footing of η). We have pointed out that, for consistency, one should use the same symmetry scheme in b_D and b_V ; nevertheless for completeness we have also considered a mixed scheme.

Nonet symmetry in the BMS model gives a good result for the slope but a too small $a_{V,0}$ and, consequently, does not accomplish our criterium of a simultaneous description of both $K_L \rightarrow \gamma \gamma^*$ and $K_L \rightarrow \pi^0 \gamma \gamma$. The WDM might describe the slope but probably gives a too small value for $a_{V,0}$ and, in any case, the dynamical mechanism underlying the theory is poorly known. The FM could describe well both the slope and $a_{V,0}$ but for a value $k_F \simeq 1$, that is, naive FM. This would imply that the enhancement of the $\Delta I = 1/2$ is at work in these channels. However our study shows that this fact is a fake of the application of the FM because, as we have found out, there is an important factorizable contribution that was missing.

We have first proposed a framework in which the full structure of the most general octet weak $VP\gamma$ vertex (with the octet of pseudoscalars) is presented. This allows us to parameterize the observables a_V and b_D in terms of five unknown effective coupling constants. Then we have applied the FM in a novel approach: we use it in order to carry the construction of the weak $VP\gamma$ vertex instead of the weak $K\pi\gamma\gamma$ or $K\gamma\gamma^*$ vertices. In this way we discover a new chiral structure contributing to both a_V and b_D that is missed in the usual approach and without including any extra incertitude in the couplings. This contribution is due to the Wess–Zumino–Witten anomaly. This procedure together with the choice of the effective coupling Eq. (92) constitutes our Factorization Model in the Vector couplings (FMV). The effective coupling Eq. (92) amounts to the bare Wilson coefficient in the non-leptonic hamiltonian and therefore no enhancement $\Delta I = 1/2$ is included in our model. As already pointed out the experimental slope of $K_L \rightarrow \gamma \gamma^*$ might prefer a slightly larger value for the coupling but probably still compatible within the error of the Wilson coefficient.

We emphasize also that it is very important to have a reliable and predictive model to establish clearly other uncertainties involved in the study of these processes (higher order corrections, large $SU(3)$ breaking, other resonance exchanges, etc.). Thus the effectiveness of the Wilson coefficient in the description of the phenomenology of these processes, we think, is a relevant step forward for a predictive description and understanding of non-leptonic kaon decays.

In Tables 1 and 2 we collect our main results for a_V and b_D and we compare them with the rest of the analysed models. We conclude that the FMV model with the new contribution that we have found gives a consistent picture of both $K \rightarrow \pi \gamma \gamma$ and $K_L \rightarrow \gamma \gamma^*$ processes and, in particular, predicts a value of $a_{V,0} = -0.72$ in rather good agreement

with the phenomenological estimate $a_{V,0} \simeq -0.8$.

We have also considered the discontinuity contribution of $K_L \rightarrow \pi^0 \gamma \gamma$ to the CP-conserving amplitude of $K_L \rightarrow \pi^0 e^+ e^-$ for our value of $a_{V,0}$. The result, given in Eq. (103), agrees with previous estimates.

Then we use our results in order to show the diphoton invariant mass spectrum of $K_L \rightarrow \pi^0 \gamma \gamma$ including the $\mathcal{O}(p^6)$ unitarity corrections from $K_L \rightarrow \pi^0 \pi^+ \pi^-$, the experimental amplitude $\gamma \gamma \rightarrow \pi^0 \pi^0$ and the vector meson contribution we have evaluated (Fig. 3 and Fig. 4). Also shown in Fig. 5 and Fig. 6 are the z -cut y -spectrum from $K_L \rightarrow \pi^0 \gamma \gamma$ and $K^+ \rightarrow \pi^+ \gamma \gamma$, respectively, that happen to be sensitive to the a_V parameter [18] and therefore worth to get from the experiments in order to clarify the subject.

For completeness we have also shown in the Appendix that our model can also be derived in the Hidden Symmetry formulation of vector mesons [27] where the phenomenological couplings are recovered in the so-called “complete vector meson dominance scheme”.

Acknowledgements

The authors thank G. Ecker, G. Isidori and A. Pich for very fruitful discussions. We also thank L. Cappiello for suggestions. J.P. is supported by an INFN Postdoctoral fellowship. J.P. is also partially supported by DGICYT under grant PB94-0080.

Appendix

We have constructed the FMV model in the frame of χ PT using the Callan–Coleman–Wess–Zumino formalism [22] for the pseudoscalar sector and the inclusion of vector mesons as matter fields with a vector field realization. We commented that the antisymmetric realization of the vector fields is less suitable in the odd-intrinsic parity sector due to simple kinematical reasons [18]. However we have found out that the realization of vector mesons in the Hidden Symmetry model [27] is as well behaved as our formulation. Its application to the study of the odd-intrinsic parity violating strong lagrangian was developed in [57, 51].

The Hidden Symmetry model relies on the property that any nonlinear sigma model based on the manifold G/H is known to be gauge equivalent to a “linear” model with $G_{global} \otimes H_{local}$ symmetry, and the gauge bosons corresponding to the hidden local symmetry, H_{local} are composite fields. In [27] was proposed that vector mesons are to be identified with the dynamical gauge bosons of hidden local $U(3)$ symmetry in the $U(3)_L \otimes U(3)_R / U(3)_V$ nonlinear sigma model.

The ideally mixed vector nonet ρ_μ ,

$$\rho_\mu = \frac{1}{\sqrt{2}} \sum_{i=1}^8 \rho_\mu^i \lambda_i + \frac{1}{\sqrt{3}} \rho_\mu^0 \quad , \quad (\text{A.1})$$

now transforms inhomogeneously under the chiral group as

$$\rho_\mu \xrightarrow{G} h \rho_\mu h^\dagger + i h \partial_\mu h^\dagger \quad , \quad h \in U(3)_V \quad (\text{A.2})$$

in contradistinction with our realization in Eq. (14).

The Lagrangian describing the vector mesons (to be added to \mathcal{L}_2 in Eq. (8)) is

$$\begin{aligned} \mathcal{L}_\rho &= a F_\pi^2 \langle (i \sigma^\dagger D_\mu \sigma)^2 \rangle - \frac{1}{4} \langle \rho_{\mu\nu} \rho^{\mu\nu} \rangle \quad , \\ i \sigma^\dagger D_\mu \sigma &\equiv i \sigma^\dagger \partial_\mu \sigma - g \sigma^\dagger \rho_\mu \sigma + v_\mu \quad , \\ \rho_{\mu\nu} &\equiv \partial_\mu \rho_\nu - \partial_\nu \rho_\mu + i g [\rho_\mu, \rho_\nu] \quad , \\ v_\mu &\equiv \frac{1}{2i} \left[\xi^\dagger (\partial_\mu - i r_\mu) \xi + \xi (\partial_\mu - i l_\mu) \xi^\dagger \right] \quad , \end{aligned} \quad (\text{A.3})$$

where a is a free parameter in the model and σ is a 3×3 unitary matrix of unphysical scalar fields. These scalars give the longitudinal component to the 3×3 vector meson matrix ρ_μ and will be gauged away fixing the unitary gauge where σ is the 3×3 identity matrix.

The relevant Lagrangian for our $PV\gamma$ vertices, that will generate the analogous to $S(VP\gamma)$ in Eq. (89) turns out to be [51]

$$\begin{aligned} \mathcal{L}_{odd}^H &= \frac{i}{2} \varepsilon^{\mu\nu\alpha\beta} \left[g a_2 \langle \sigma^\dagger \rho_{\mu\nu} \sigma \{ a_\alpha, \sigma^\dagger D_\beta \sigma \} \rangle \right. \\ &\quad \left. - a_3 \langle (\xi F_{\mu\nu}^L \xi^\dagger + \xi^\dagger F_{\mu\nu}^R \xi) \{ a_\alpha, \sigma^\dagger D_\beta \sigma \} \rangle \right] \quad . \end{aligned} \quad (\text{A.4})$$

In the unitary gauge $\sigma \rightarrow I$ and then $\xi \rightarrow u$ and $a_\mu \rightarrow u_\mu$ defined in Eq. (9). Three new coupling constants appear in \mathcal{L}_{odd}^H : g , a_2 and a_3 . g is the gauge coupling associated to the hidden symmetry and it can be evaluated from $\Gamma(\rho \rightarrow \pi\pi)$ as $|g| = m_V/(2F_\pi) \simeq 4.1$, a_2 and a_3 can be determined from the strong $V \rightarrow P\gamma$ processes. The phenomenology of these and Vector Meson Dominance is consistent with the choices [51]

$$\begin{aligned} a_2 &= 2 a_3 \simeq -\frac{3}{16\pi^2} \quad , \\ a &= 2 \quad , \end{aligned} \quad (\text{A.5})$$

(see however [58]) which induces the so-called ‘‘complete vector meson dominance’’ [57]. From \mathcal{L}_{odd}^H and comparing with Eq. (15) we can express h_V in terms of the couplings appearing in this formalism. We get

$$h_V = -\frac{1}{2} g a_2 \simeq 3.9 \times 10^{-2} \quad , \quad (\text{A.6})$$

in very good agreement with the phenomenological value $|h_V| = (3.7 \pm 0.3) \times 10^{-2}$.

In the Hidden Symmetry model the coupling $\rho\gamma$ is generated by the first term of \mathcal{L}_ρ in Eq. (A.3). By comparison and using the relation $m_V = 2gF_\pi$ (that also arises in the model) we find [26]

$$f_V = \frac{1}{\sqrt{2}g} \simeq 0.17 \quad , \quad (\text{A.7})$$

to compare with the phenomenological value $|f_V| \simeq 0.20$. We note that $h_V f_V > 0$ as indicated by phenomenology. See Section 2.1.

From Eq. (93), the expressions for h_V and f_V and the value of a_2 we get

$$\ell_V = -\frac{1}{\sqrt{2}} a_2 f_V \frac{m_V^2}{F_\pi^2} = 4 h_V \quad , \quad (\text{A.8})$$

verified phenomenologically within an error of $\sim 20\%$.

Therefore, analogously to Eq. (89) we can construct the effective actions of our interest in this model and then carry out the same application of our FMV model. As commented in the text the results are consistent in both procedures.

References

- [1] S. Weinberg, *Physica*, **96A** (1979) 327.
- [2] J. Gasser, H. Leutwyler, *Ann. of Phys.*, **158** (1984) 142,
J. Gasser, H. Leutwyler, *Nucl. Phys.*, **B250** (1985) 465.
- [3] A.V. Manohar, H. Georgi, *Nucl. Phys.*, **B234** (1984) 189.
- [4] G. Ecker, J. Gasser, A. Pich, E. de Rafael, *Nucl. Phys.*, **B321** (1989) 311.
- [5] J.F. Donoghue, C. Ramirez, G. Valencia, *Phys. Rev.*, **D39** (1989) 1947.
- [6] G. D'Ambrosio, G. Ecker, G. Isidori, H. Neufeld, "Radiative non-leptonic kaon decays" in the Second DAΦNE Physics Handbook, ed. by L. Maiani, G. Pancheri, N. Paver, LNF (1995), p. 265.
- [7] E. de Rafael, "Chiral Lagrangians and Kaon CP-violation", Lectures given at the 1994th TASI School on CP violation and the limits of the Standard Model, Univ. of Colorado at Boulder (1995).
- [8] G. D'Ambrosio, G. Isidori, "CP violation in Kaon decays", Preprint INFNNA-IV-96/29, LNF-96/033(P), submitted to *Int. J. of Mod. Phys. A*, (1996).
- [9] Novikov, V.A., Shifman, M.A., Vainshtein, A.I., Zakharov, V.I., *Phys. Rev.*, **D16** (1977) 223,
Ellis, J., Hagelin, J.S., *Nucl. Phys.*, **B217** (1983) 189,
Buchalla, G., Buras, A.J., *Nucl. Phys.*, **B412** (1994) 106.
- [10] L. Bergström, E. Massó, P. Singer, *Phys. Lett.*, **B131** (1983) 229, **B249** (1990) 141.
- [11] J.F. Donoghue, B.R. Holstein, G. Valencia, *Phys. Rev.*, **D35** (1987) 2769.
- [12] L. M. Sehgal, *Phys. Rev.*, **D38** (1988) 808.
- [13] J. Flynn, L. Randall, *Nucl. Phys.*, **B326** (1989) 31,
C. Dib, I. Dunietz, F.J. Gilman, *Phys. Lett.*, **B218** (1989) 487.
- [14] L. Cappiello, G. D'Ambrosio, M. Miragliuolo, *Phys. Lett.*, **B298** (1993) 423.
- [15] A. G. Cohen, G. Ecker, A. Pich, *Phys. Lett.*, **B304** (1993) 347.
- [16] Talk presented by Takao Shinkawa at the *Workshop on K-Physics*, Orsay, France, 30 May – 4 June, (1996).

- [17] G. D'Ambrosio, J. Portolés, “Unitarity and vector meson contributions to $K^+ \rightarrow \pi^+ \gamma \gamma$ ”, Preprint INFNNA-IV-96/12. DSFNA-IV-96/12, hep-ph/9606213, to be published in *Phys. Lett. B*, (1996).
- [18] G. Ecker, A. Pich, E. de Rafael, *Phys. Lett.*, **B237** (1990) 481.
- [19] G. Ecker, “Geometrical Aspects of the Non-Leptonic Weak Interactions of Mesons”, in Proc. of the IX International Conference on the Problems of Quantum Field Theory, April 24–28, (1990), Dubna, USSR.
- [20] A. Pich, E. de Rafael, *Nucl. Phys.*, **B358** (1991) 311.
- [21] P. Ko, *Phys. Rev.*, **D44** (1991) 139.
- [22] S. Coleman, J. Wess, B. Zumino, *Phys. Rev.*, **177** (1969) 2239,
C.G. Callan, S. Coleman, J. Wess, B. Zumino, *Phys. Rev.*, **177** (1969) 2247.
- [23] J. Wess, B. Zumino, *Phys. Lett.*, **B37** (1971) 95,
E. Witten, *Nucl. Phys.*, **B223** (1983) 422.
- [24] H.W. Fearing, S. Scherer, *Phys. Rev.*, **D53** (1996) 315.
- [25] Review of Particle Properties, R.M. Barnett et al., *Phys. Rev.*, **D54** (1996) 1.
- [26] G. Ecker, J. Gasser, H. Leutwyler, A. Pich, E. de Rafael, *Phys. Lett.*, **B223** (1989) 425.
- [27] M. Bando, T. Kugo, K. Yamawaki, *Phys. Rep.*, **164** (1988) 217.
- [28] J.F. Donoghue, E. Golowich, B.R. Holstein, “Dynamics of the Standard Model”, Cambridge University Press, (1992).
- [29] G. Ecker, *Prog. Part. Nucl. Phys.*, **35** (1995) 1.
- [30] A. Pich, *Rept. Prog. Phys.*, **58** (1995) 563.
- [31] M. Ciuchini, E. Franco, G. Martinelli, L. Reina, “Estimates of ε'/ε ” in the Second DAΦNE Physics Handbook, ed. by L. Maiani, G. Pancheri, N. Paver, LNF (1995) p. 27.
- [32] G. Buchalla, A.J. Buras, M.E. Lautenbacher, “Weak decays beyond leading logarithms”, MPI-Ph/95-104, to appear in *Rev. of Mod. Phys.*, (1996).
- [33] M.A. Shifman, A.I. Vainshtein, V.I. Zakharov, *Nucl. Phys.*, **B120** (1977) 316.
- [34] M.K. Gaillard, B.W. Lee, *Phys. Rev. Lett.*, **33** (1974) 108.

- [35] G. Altarelli, L. Maiani, *Phys. Lett.*, **B52** (1974) 351.
- [36] J. Kambor, J. Missimer, D. Wyler, *Phys. Lett.*, **B261** (1991) 496.
- [37] J. Kambor, J. Missimer, D. Wyler, *Nucl. Phys.*, **B346** (1990) 17.
- [38] G. Ecker, J. Kambor, D. Wyler, *Nucl. Phys.*, **B394** (1993) 101.
- [39] G. Isidori, A. Pugliese, *Nucl. Phys.*, **B385** (1992) 437.
- [40] G. Ecker, H. Neufeld, A. Pich, *Nucl. Phys.*, **B413** (1994) 321.
- [41] G. Ecker, A. Pich, E. de Rafael, *Nucl. Phys.*, **B303** (1988) 665.
- [42] G. D'Ambrosio, G. Isidori, *Z. Phys.*, **C65** (1995) 649.
- [43] J.F. Donoghue, F. Gabbiani, *Phys. Rev.*, **D51** (1995) 2187.
- [44] G. Ecker, A. Pich, E. de Rafael, *Phys. Lett.*, **B189** (1987) 363,
L. Cappiello, G. D'Ambrosio, *Nuovo Cimento*, **99A** (1988) 155.
- [45] C. Bruno, J. Prades, *Z. Phys.*, **C57** (1993) 585.
- [46] G.D. Barr et al, *Phys. Lett.*, **B242** (1990) 523, **B284** (1992) 440.
- [47] V. Papadimitriou et al. *Phys. Rev.*, **D44** (1991) 573.
- [48] L.M. Sehgal, *Phys. Rev.*, **D41** (1990) 161,
P. Heiliger, L.M. Sehgal, *Phys. Rev.*, **D47** (1993) 4920.
- [49] J. Kambor, B.R. Holstein, *Phys. Rev.*, **D49** (1994) 2346.
- [50] G. Ecker, “Chiral Realization of the Non-Leptonic Weak Interactions”, in Proc. of the XXIV International Symposium on the Theory of Elementary Particles, October 8-12, 1990, Gosen (Berlin), Germany.
- [51] J. Bijnens, A. Bramon, F. Cornet, *Z. Phys.*, **C46** (1990) 599.
- [52] K.E. Ohl et al., *Phys. Rev. Lett.*, **65** (1990) 1407,
G.D. Barr et al, *Phys. Lett.*, **B240** (1990) 283.
- [53] M.B. Spencer et al, *Phys. Rev. Lett.*, **74** (1995) 3323.
- [54] M.K. Gaillard, B.W. Lee, *Phys. Rev.*, **D10** (1974) 897,
E. Ma, A. Pramudita, *Phys. Rev.*, **D24** (1981) 2476.

- [55] G. D'Ambrosio, D. Espriu, *Phys. Lett.*, **B175** (1986) 237,
 J.F. Donoghue, B.R. Holstein, Y.-C.R. Lin, *Nucl. Phys.*, **B277** (1986) 651,
 J. I. Goity, *Z. Phys.*, **C34** (1987) 341,
 L.L. Chau, H.-Y Cheng, *Phys. Rev. Lett.*, **54** (1985) 1768; *Phys. Lett.*, **B195** (1987) 275 ,
 F. Buccella, G. D'Ambrosio, M. Miragliuolo, *Nuovo Cimento*, **104A** (1991) 777.
- [56] J. Bijnens, G. Ecker, A. Pich, *Phys. Lett.*, **B286** (1992) 341.
- [57] T. Fujikawa, T. Kugo, H. Terao, S. Uehara, K. Yamawaki, *Progr. of Theor. Phys.*, **73** (1985) 926.
- [58] A. Bramon, A. Grau, G. Pancheri, “Vector Meson Decays in Effective Chiral Lagrangians” in The Second DAΦNE Physics Handbook, ed. by L. Maiani, G. Pancheri, N. Paver, LNF (1995), p. 477.
 See also
 A. Bramon, A. Grau, E. Pallante, G. Pancheri, R. Petronzio, “The effective photon–pseudoscalar anomalous interactions: $e^+e^- \rightarrow \pi^+\pi^-\pi^0$, $\pi^0\gamma$, $\eta\gamma$, $\pi^0\gamma^{*}$ ”, in The DAΦNE Physics Handbook, ed. by L. Maiani, G. Pancheri, N. Paver, LNF (1992), p. 305.